

A Large Ion Collider Experiment



ALICE

ALICE status report

Silvia Pisano

Laboratori Nazionali di Frascati - INFN

on behalf of

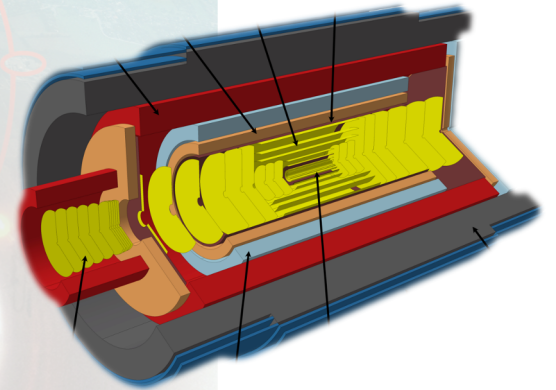
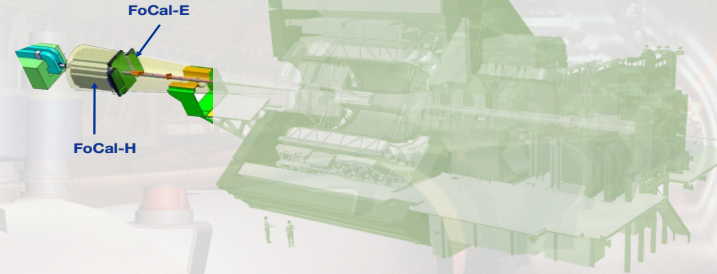
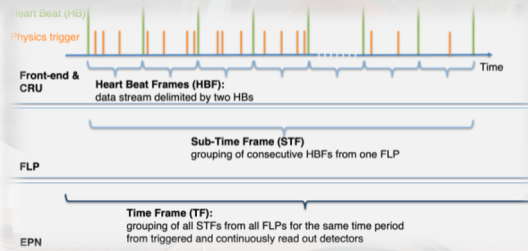
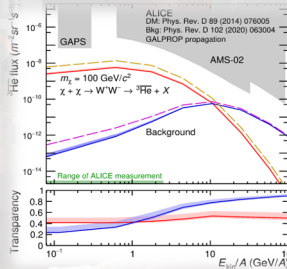
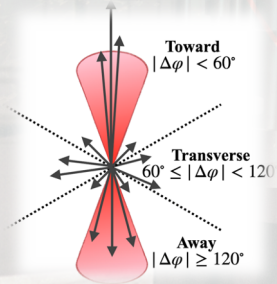
The ALICE Collaboration

LHCC Open Session – Wednesday March 8^o, 2023

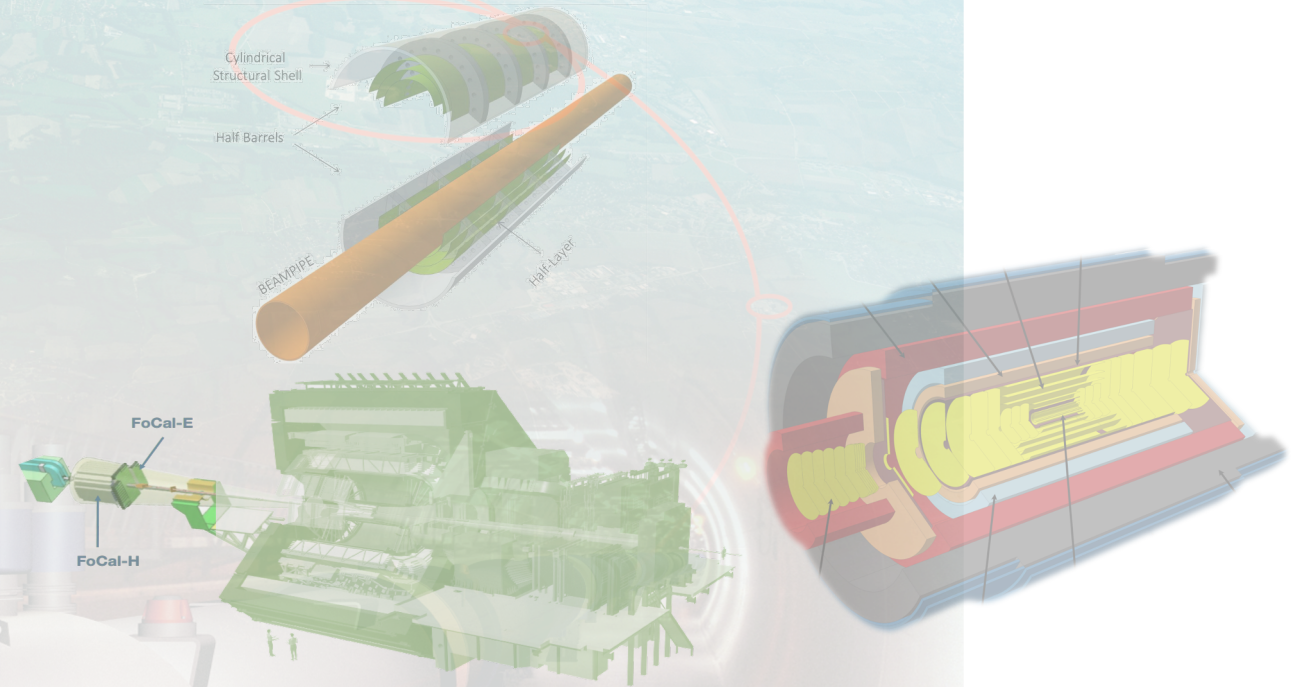
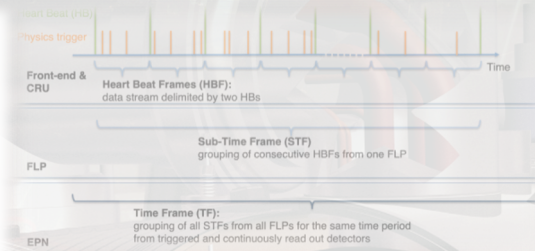
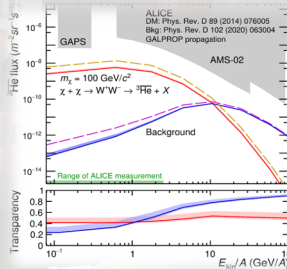
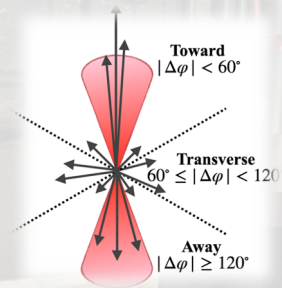
Contents



1. Latest publications and selected physics results
2. Data taking in 2023
3. ALICE + ITS3 & FoCal
4. ALICE 3 upgrade



1. Latest publications and selected physics results
2. Data taking in 2023
3. ALICE + ITS3 & FoCal
4. ALICE 3 upgrade



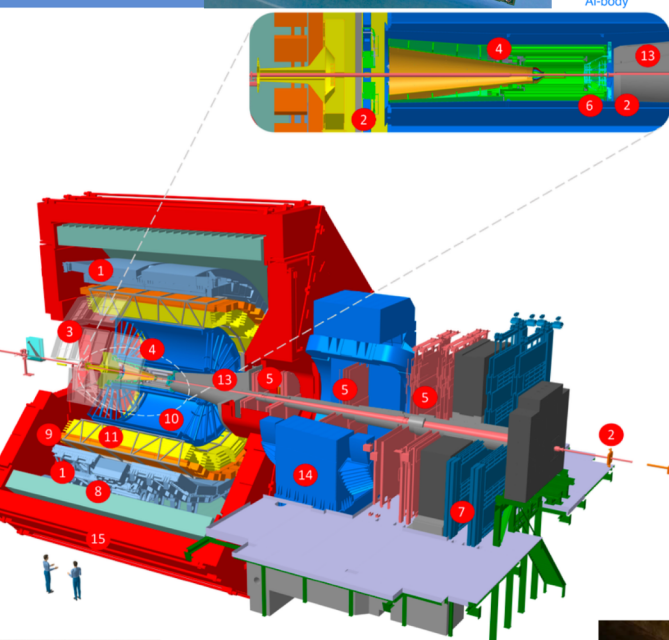
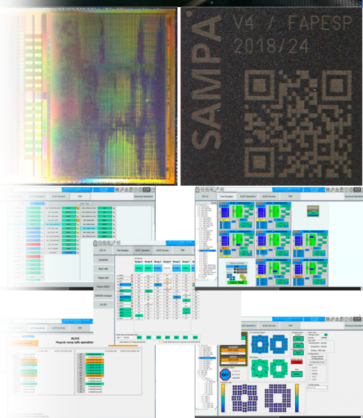
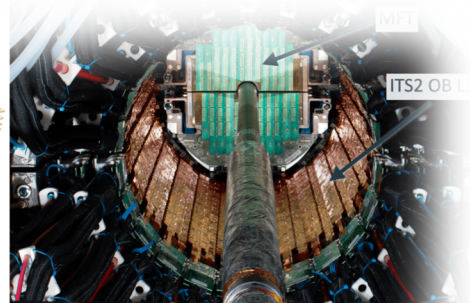
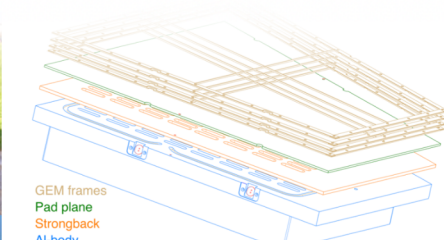
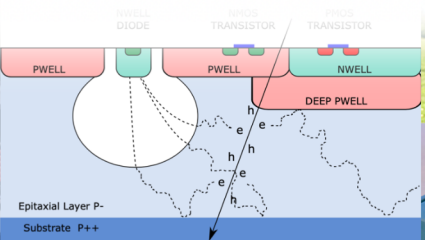
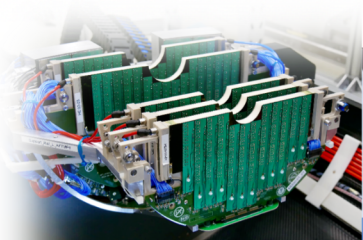
New publications since last LHCC



1. [Pseudorapidity densities of charged particles with transverse momentum thresholds in pp collisions at \$\sqrt{s} = 5.02\$ and 13 TeV, arXiv:2211.15364](#)
2. [Production of pions, kaons and protons as a function of the transverse event activity in pp collisions at \$\sqrt{s} = 13\$ TeV, arXiv:2301.10120](#)
3. [Measurement of \(anti\)nuclei production in p-Pb collisions at \$\sqrt{s_{NN}} = 8.16\$ TeV, arXiv:2212.04777](#)
4. [First measurement of prompt and non-prompt \$D^{*+}\$ vector meson spin alignment in pp collisions at \$\sqrt{s} = 13\$ TeV, arXiv:2212.06588](#)
5. [Azimuthal anisotropy of jet particles in p-Pb and Pb-Pb collisions at \$\sqrt{s_{NN}} = 5.02\$ TeV, arXiv:2212.12609](#)
6. [Exploring the non-universality of charm hadronisation through the measurement of the fraction of jet longitudinal momentum carried by \$\Lambda_c^+\$ baryons in pp collisions, arXiv:2301.13798](#)
7. [Symmetry plane correlations in Pb-Pb collisions at \$\sqrt{s_{NN}} \equiv 2.76\$ TeV, arXiv:2302.01234](#)
8. [Measurement of the non-prompt D-meson fraction as a function of multiplicity in proton-proton collisions at \$\sqrt{s} = 13\$ TeV, arXiv:2302.07783](#)
9. [Neutron emission in ultraperipheral Pb-Pb collisions at \$\sqrt{s_{NN}} = 5.02\$ TeV, arXiv:2209.04250](#)
10. [Light \(anti\)nuclei production in Pb-Pb collisions at \$\sqrt{s} = 5.02\$ TeV, arXiv:2211.14015](#)
11. [Measurement of \(anti\)nuclei production in p-Pb collisions at \$\sqrt{s_{NN}} = 8.16\$ TeV, arXiv:2212.0477](#)
12. [Measurement of the \$\Lambda\$ hyperon lifetime, arXiv:2303.00606](#)
13. [Azimuthal correlations of heavy-flavor hadron decay electrons with charged particles in pp and p-Pb collisions at \$\sqrt{s} = 5.02\$ TeV, arXiv: 2303.00591](#)
14. [Inclusive photon production at forward rapidities in pp and p-Pb collisions at \$\sqrt{s} = 5.02\$ TeV, arXiv: 2303.00590](#)
15. [Measurement of the radius dependence of charged-particle jet suppression in Pb-Pb collisions at \$\sqrt{s} = 5.02\$ TeV, arXiv: 2303.0059092](#)
16. [ALICE upgrades during the LHC Long Shutdown 2, arXiv:2302.01238](#)

ALICE upgrades during the LHC Long Shutdown 2

arXiv:2302.01238, submitted to JINST, as part of a Special Issue on LHC and experiments upgrades during LS2



- 1 EMCAL | Electromagnetic Calorimeter
- 2 FIT | Fast Interaction Trigger
- 3 HMPID | High Momentum Particle Identification Detector
- 4 ITS | Inner Tracking System
- 5 MCH | Muon Tracking Chambers
- 6 MFT | Muon Forward Tracker
- 7 MID | Muon Identifier
- 8 PHOS/CPV | Photon Spectrometer
- 9 TOF | Time Of Flight
- 10 TPC | Time Projection Chamber
- 11 TRD | Transition Radiation Detector
- 12 ZDC | Zero Degree Calorimeter
- 13 Absorber
- 14 Dipole Magnet
- 15 L3 Magnet

EUROPEAN ORGANIZATION FOR NUCLEAR RESEARCH



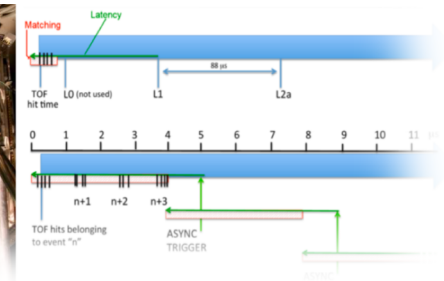
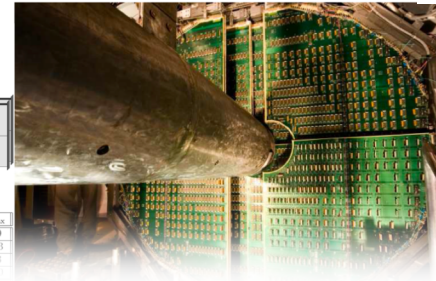
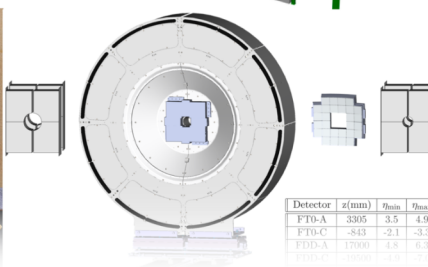
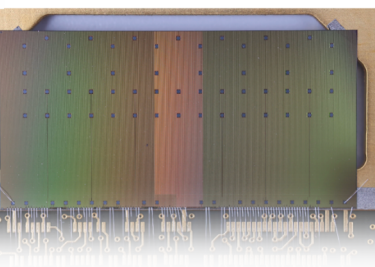
CERN-EP-2023-009
27 January 2023

ALICE upgrades during the LHC Long Shutdown 2

ALICE Collaboration

Abstract

Overview paper on the
ALICE upgrades in LS2!



ALICE estimates transparency of the Milky Way to antimatter

[Nature Physics volume 19, 61 \(2023\)](#)



Measurement of $\overline{^3\text{He}}$ absorption cross section and implications for interpretation of potential dark annihilation signals

nature physics



Article

<https://doi.org/10.1038/s41567-022-01804-8>

Measurement of anti- ^3He nuclei absorption in matter and impact on their propagation in the Galaxy

Received: 18 February 2022

Accepted: 21 September 2022

Published online: 12 December 2022

 Check for updates

The ALICE Collaboration* 

In our Galaxy, light antinuclei composed of antiprotons and antineutrons can be produced through high-energy cosmic-ray collisions with the interstellar medium or could also originate from the annihilation of dark-matter particles that have not yet been discovered. On Earth, the only way to produce and study antinuclei with high precision is to create them at high-energy particle accelerators. Although the properties of elementary antiparticles have been studied in detail, the knowledge of the interaction of light antinuclei with matter is limited. We determine the disappearance probability of $^3\overline{\text{He}}$ when it encounters matter particles and annihilates or disintegrates within the ALICE detector at the Large Hadron Collider. We extract the inelastic interaction cross section, which is then used as an input to the calculations of the transparency of our Galaxy to the propagation of $^3\overline{\text{He}}$ stemming from dark-matter annihilation and cosmic-ray interactions within the interstellar medium. For a specific dark-matter profile, we estimate a transparency of about 50%, whereas it varies with increasing $^3\overline{\text{He}}$ momentum from 25% to 90% for cosmic-ray sources. The results indicate that $^3\overline{\text{He}}$ nuclei can travel long distances in the Galaxy, and can be used to study cosmic-ray interactions and dark-matter annihilation.



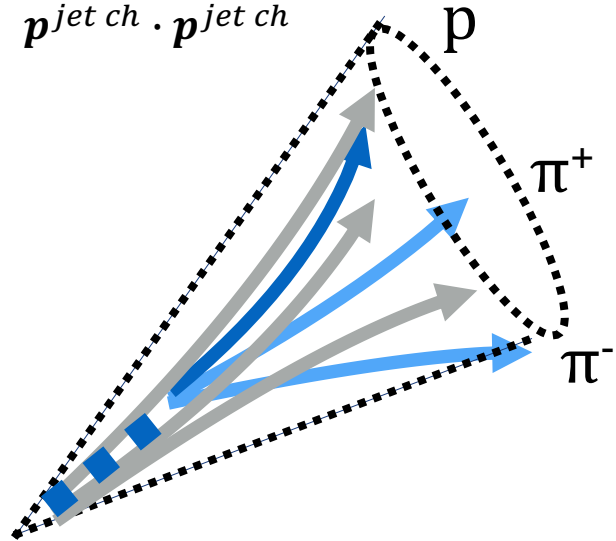
Published
in
Nature
Physics!

LHCC Open Session - March 8th, 2023

First measurement of the Λ_c fragmentation in pp

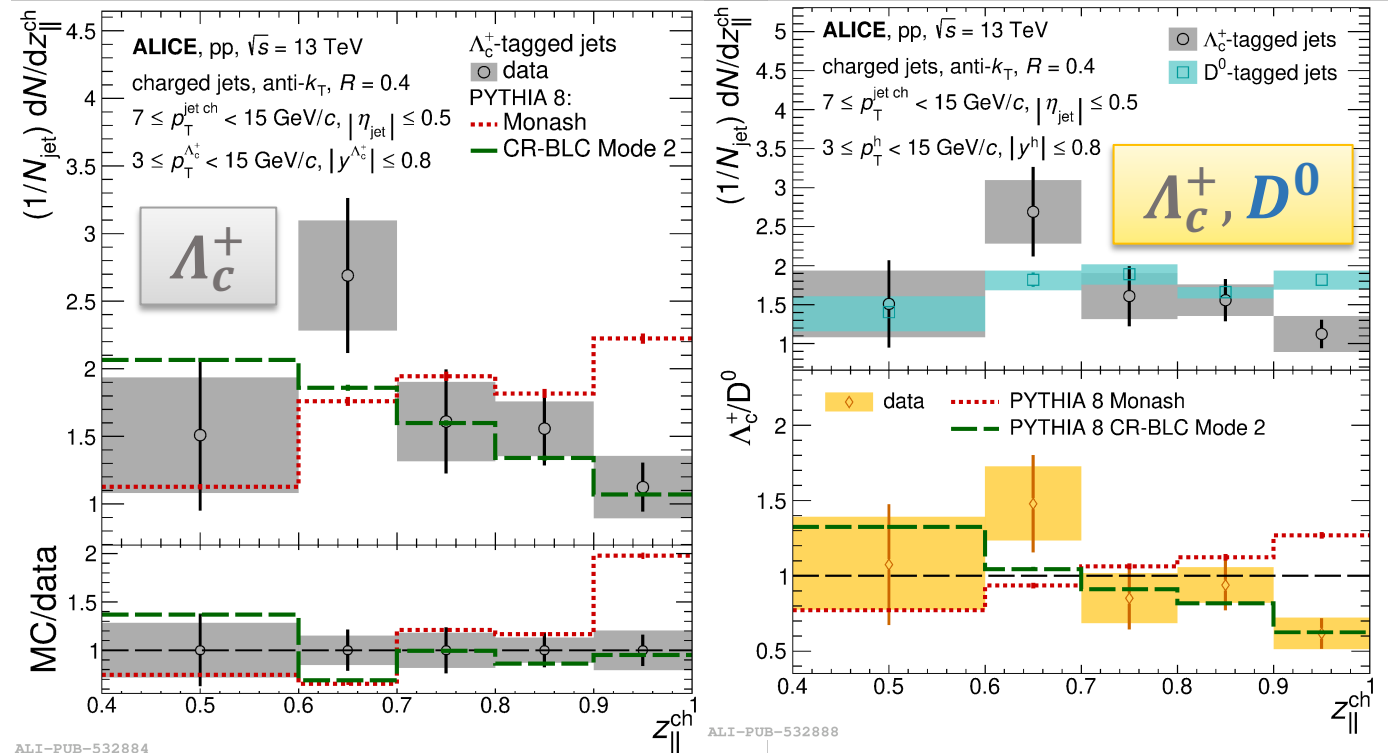
Longitudinal momentum fraction carried by the Λ_c^+

$$z_{\parallel}^{ch} = \frac{\mathbf{p}^{jet\ ch} \cdot \mathbf{p}^{HF}}{\mathbf{p}^{jet\ ch} \cdot \mathbf{p}^{jet\ ch}}$$



c quark

[arXiv: 2301.13798](https://arxiv.org/abs/2301.13798)



First measurement of Λ_c^+ fragmentation properties in hadronic collisions:

- Hint of softer fragmentation pattern than predicted by PYTHIA with leading-order string fragmentation (e.g. Monash)
- New constraints on the enhancement of charmed baryon production in pp collisions

Azimuthal anisotropy of jet particles

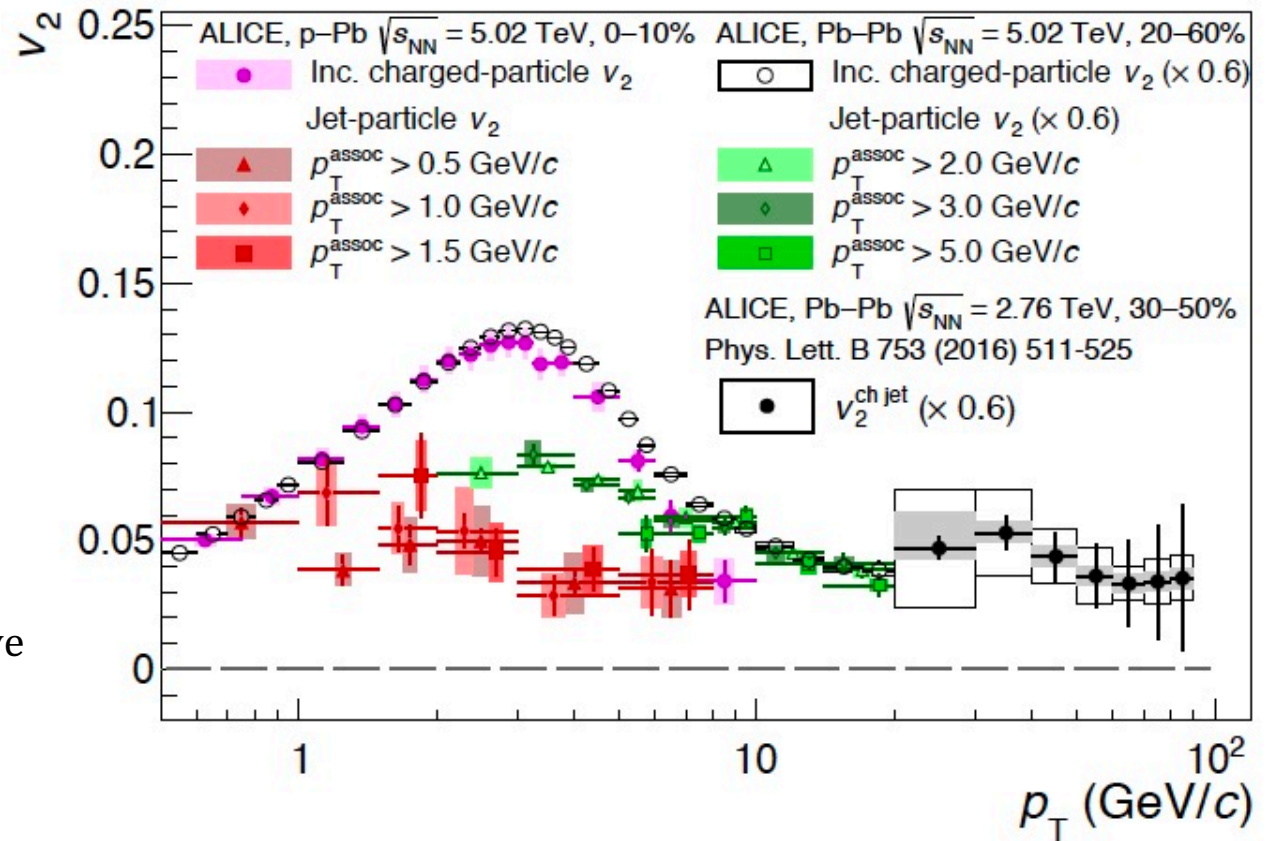
[arXiv: 2212.12609](https://arxiv.org/abs/2212.12609)

Long-standing puzzle: *collective effects observed in small collision systems, but no signs of jet quenching*

- First measurement of jet-particle v_2 in high-multiplicity p-Pb collisions at low $p_T = (0.5 - 8.0)$ GeV/c

$$\frac{d^2N}{dp_T d\phi} = \frac{1}{2\pi} \frac{dN}{dp_T} \left(1 + 2 \sum_{n=1}^{\infty} v_n(p_T) \cos[n(\phi - \Psi_n)] \right)$$

- No dependence on p_T is observed (while the inclusive charged-particle v_2 shows a clear dependence).

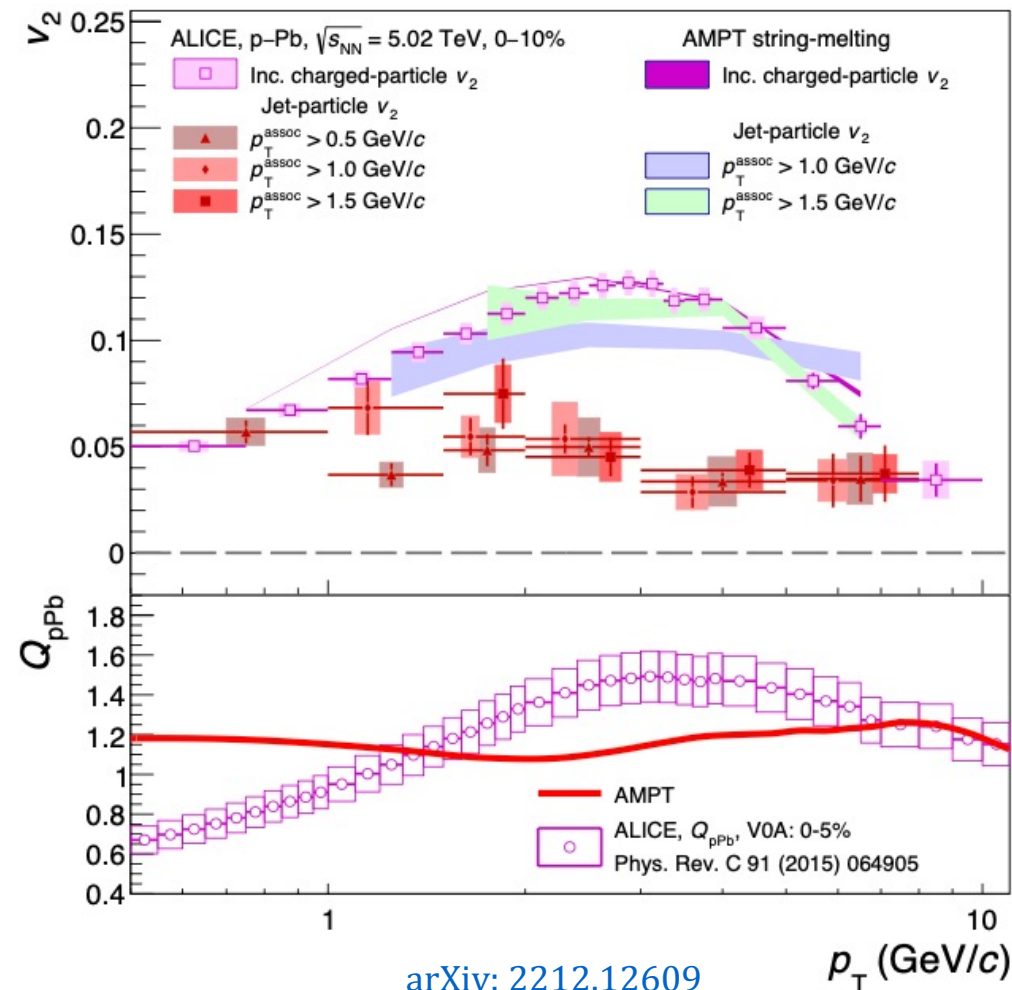


Azimuthal anisotropy of jet particles

Long-standing puzzle: *collective effects observed in small collision systems, but no signs of jet quenching*

AMPT (A MultiPhase Transport model):

1. overestimates the measured jet-particle v_2 , predicting a shape and magnitude compatible with those of inclusive charged particles (all final state particles generated with HIJING are treated on equal footing)
2. AMPT predicts significant v_2 with only few parton-parton scatterings, while preserving Q_{pPb} (in the region where usually jet quenching is observed, i.e. $p_T > 7$ GeV/c)



[arXiv: 2212.12609](https://arxiv.org/abs/2212.12609)

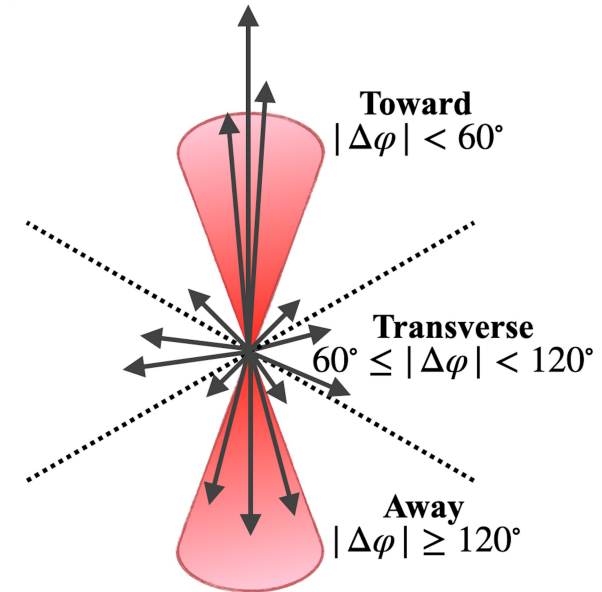
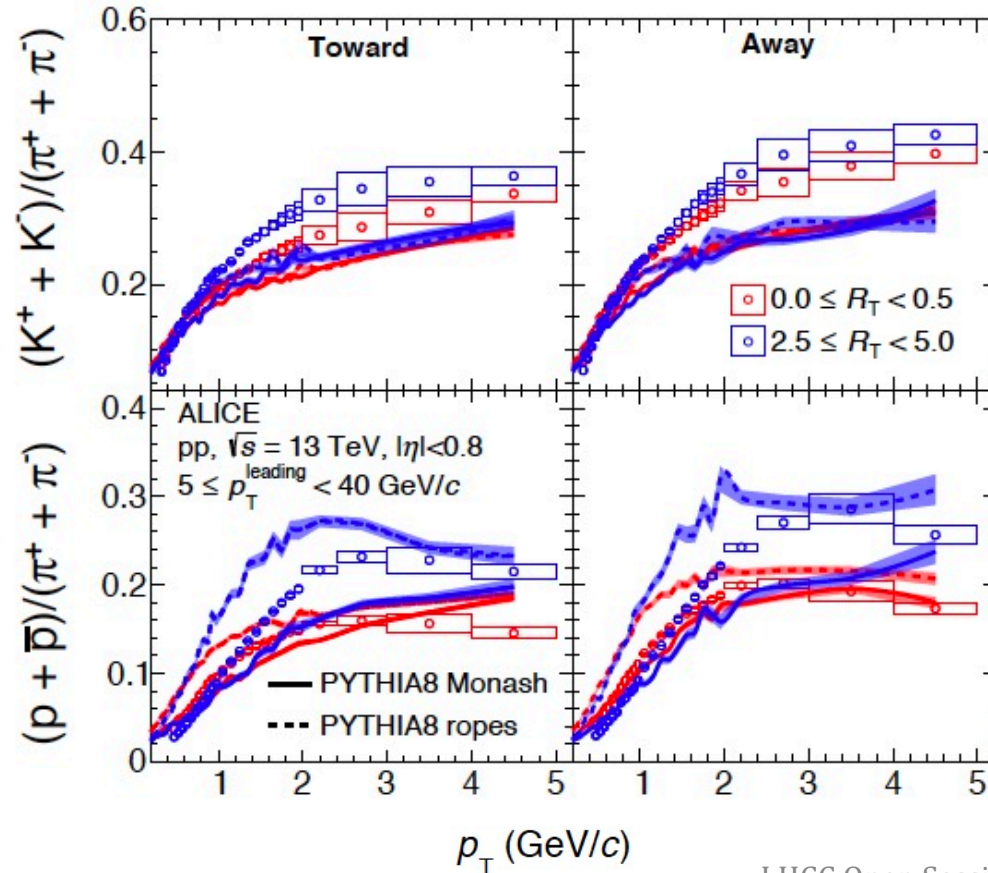
Identified particle production vs. R_T

[arXiv: 2301.10120](https://arxiv.org/abs/2301.10120)



Relative transverse activity classifier, underlying event multiplicity :

$$R_T = N_{ch}^{transverse} / \langle N_{ch}^{transverse} \rangle$$



Increase of p/π ratio at moderate and high p_T at large R_T

No effect in PYTHIA Monash; PYTHIA ropes show qualitatively similar effect

Particle production in jets and underlying event not independent: density effects in pp?

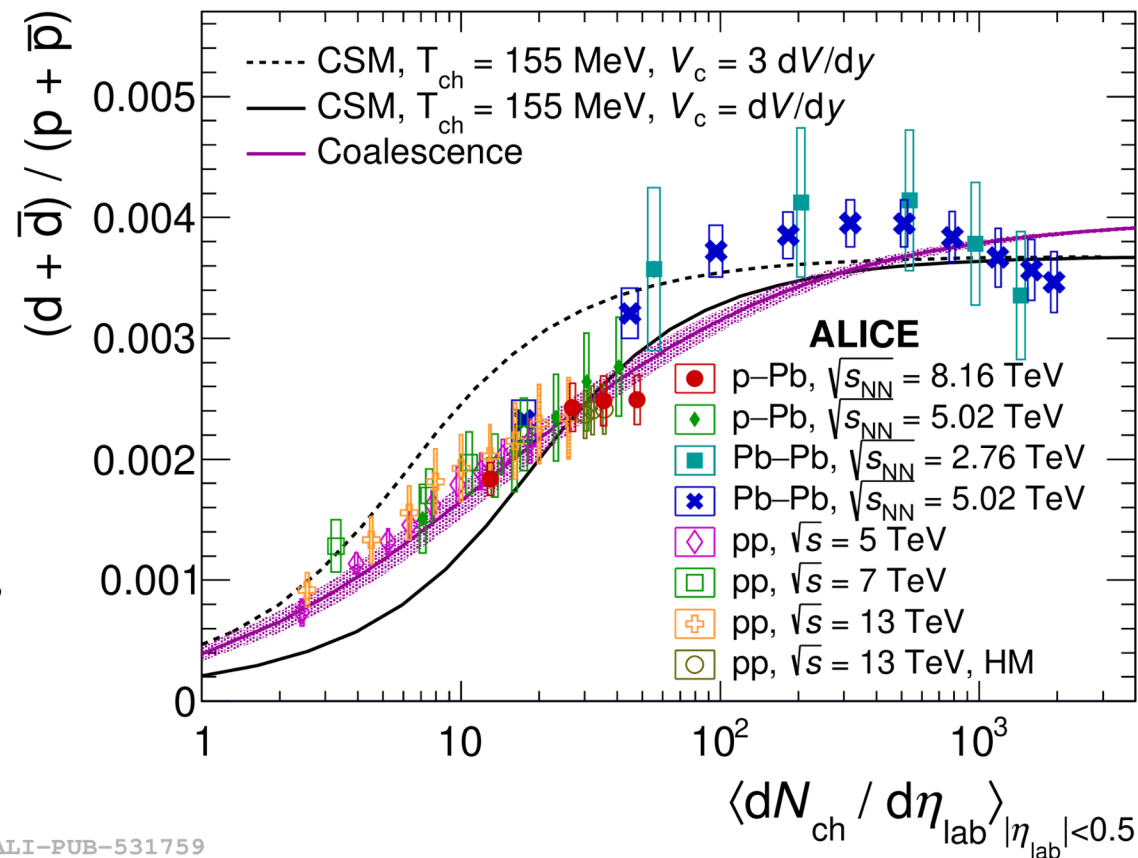
Antinuclei production from small to large systems

[arxiv: 2211.14015](https://arxiv.org/abs/2211.14015), [arxiv: 2212.04777](https://arxiv.org/abs/2212.04777)

How (anti-)nuclei are formed in high-energy collisions, and how they survive in the post hadronization phase?

Two main models: statistical hadronization model and coalescence → discriminate using system size dependence of deuteron yields

1. **Coalescence model:** evolution of the d/p ratio *well described* over the full multiplicity interval
2. **Canonical statistical model (CSM):** *consistent with the Pb-Pb measurements at $\sqrt{s_{NN}} = 2.76$ TeV and $\sqrt{s_{NN}} = 5.02$ TeV within the uncertainties, describing the plateau at the highest multiplicities. At lower multiplicities better agreement with coalescence model.*



ALI-PUB-531759

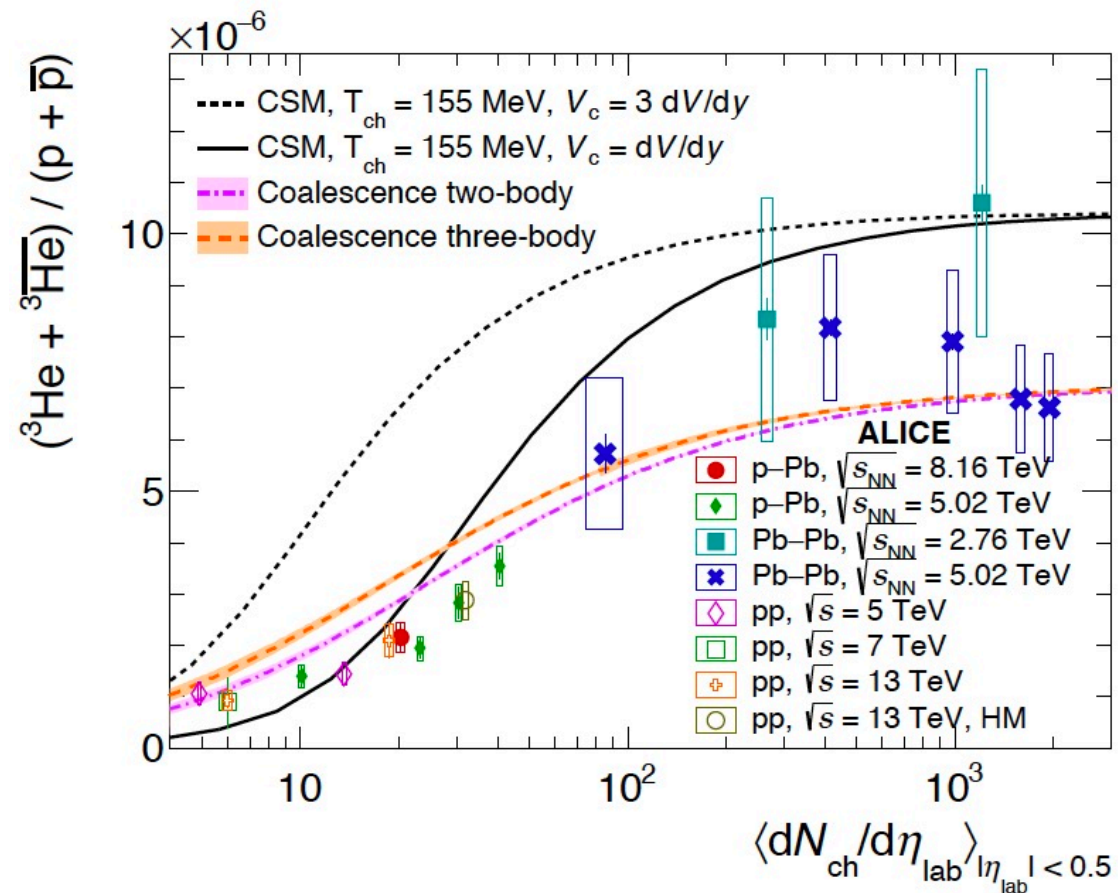
Antinuclei production from small to large systems

[arxiv: 2211.14015](https://arxiv.org/abs/2211.14015), [arxiv: 2212.04777](https://arxiv.org/abs/2212.04777)

How (anti-)nuclei are formed in high-energy collisions, and how they survive in the post hadronization phase?

Two main models: statistical hadronization model and coalescence → discriminate using system size dependence of deuteron yields

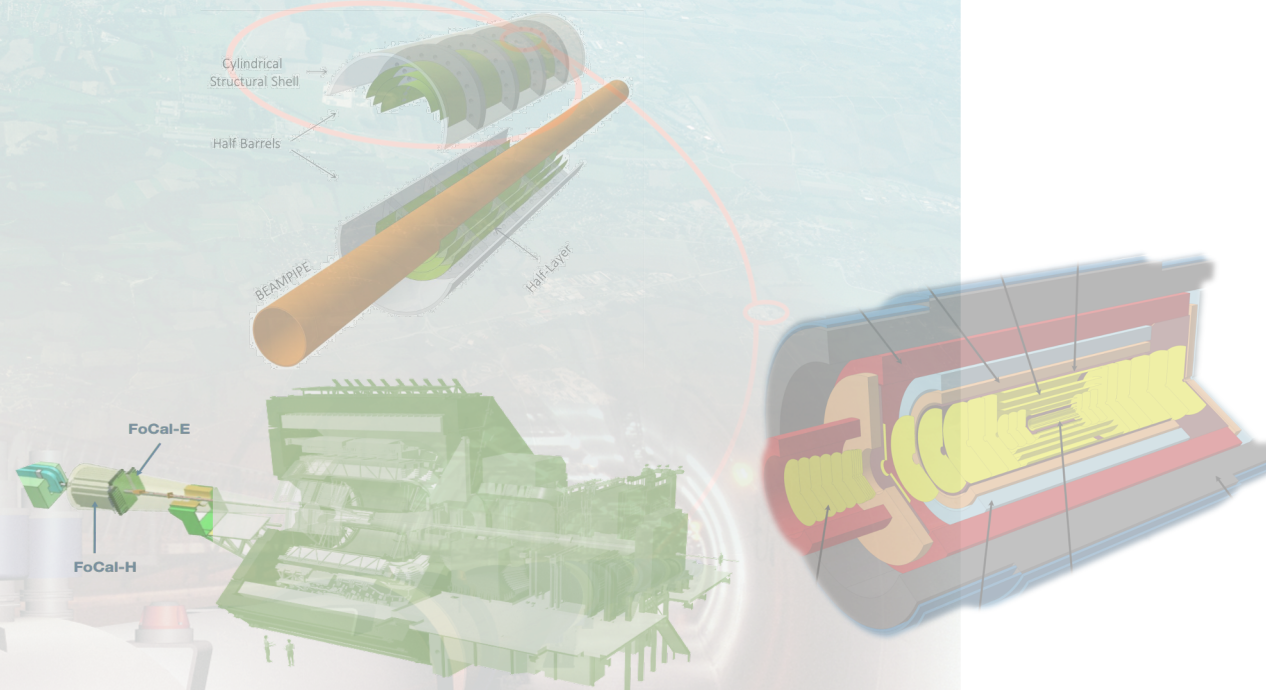
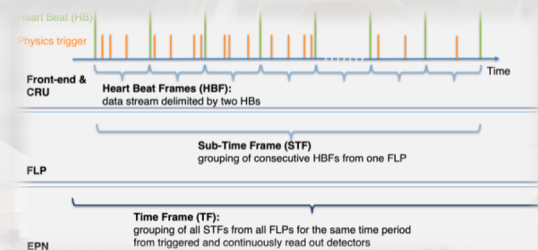
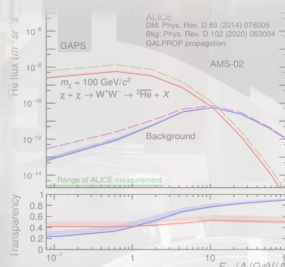
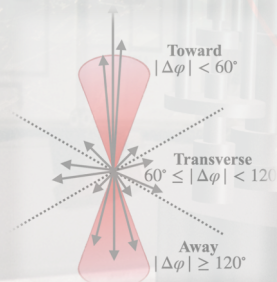
1. **Coalescence model:** *well described* at low and intermediate charged-particle multiplicity densities, while predictions underestimate the data at high multiplicities
2. **Canonical statistical model (CSM):** *only qualitative agreement* at low and intermediate multiplicities, while describing the plateau at the highest multiplicities.



Institute affiliations on author list

- In response to the invasion of Ukraine by the Russian Federation, the LHC experiments postponed publications in journals
- Discussions of institutional acknowledgement on publications resulted in a joint decision by Collaboration Boards of the four large experiments:
 1. *Authors affiliated with Russian or Belarussian institutes, or with JINR, sign the Collaboration's scientific publications with their names and ORCID identifiers (where available), and the institute affiliation is replaced, respectively, by the reference:
"Affiliated with an institute [or an international laboratory] covered by a cooperation agreement with CERN."
The complete author list including all institute affiliations is made available to the journal in a non-public form for the purpose of machine-readable analysis or as historical data.*
 2. *No acknowledgement to the Russian and Belarussian funding agencies and JINR is made. On request, the experiment management will release a certificate attesting the contribution of the aforementioned institutes and funding agencies, or of JINR, to the work presented in the publication.*
- Implementation of this decision in progress
 - Journals contacted, expect to resume publications soon
 - Collection of ORCIDs for all authors ongoing

1. Latest publications and selected physics results
2. **Data taking in 2023**
3. ALICE + ITS3 & FoCal
4. ALICE 3 upgrade



Data taking in 2023



March 6° – September 17° : pp

- Magnet scans
- High-rate scan for Pb-Pb preparation:
 1. *Regular scan up to 4 MHz (equivalent Pb-Pb 50 kHz track load)*
 2. *Improve detector conditioning to trip (TPC, MCH, TRD)*
 3. *Commission the TPC firmware*

September 17° - October 1°: pp reference

October 2° - October 30°: Pb-Pb

Objectives	Magnet polarity Solenoid / Dipole	Magnet field Solenoid / Dipole	Interaction rate	Run ning time
Test low field reco in preparation for Pb-Pb	+/+	+12kA / +6 kA (low field*)	500 kHz	6h
Calibration	+/+	+12kA / +6 kA (low field*)	5-10 Khz	~2h
Alignement	0/0	0/0	5-10 Khz	6h
Calibration	-/-	-12kA / -6 kA (low field*)	5-10 Khz	~2h
Test low field reco in preparation for Pb-Pb	-/-	-12kA / -6 kA (low field*)	500 kHz	6h

* Nominal Magnet field configuration : +30kA/+6 kA

Performance results with 2022 data

Reconstruction and calibration of the 2022 pp data

1. CTF skimming → *Data skimming with offline trigger*
2. Both standard grid nodes with CPUs and the EPN farm with GPUs are being used.

Latest results on reconstructed 2022 shows that the main observable are reaching their nominal values

- Impact parameter resolution close to the nominal values
- dE/dx back to nominal Bethe-Bloch values
- Good reconstruction of both neutral and charged decays through EMCAL and muon systems

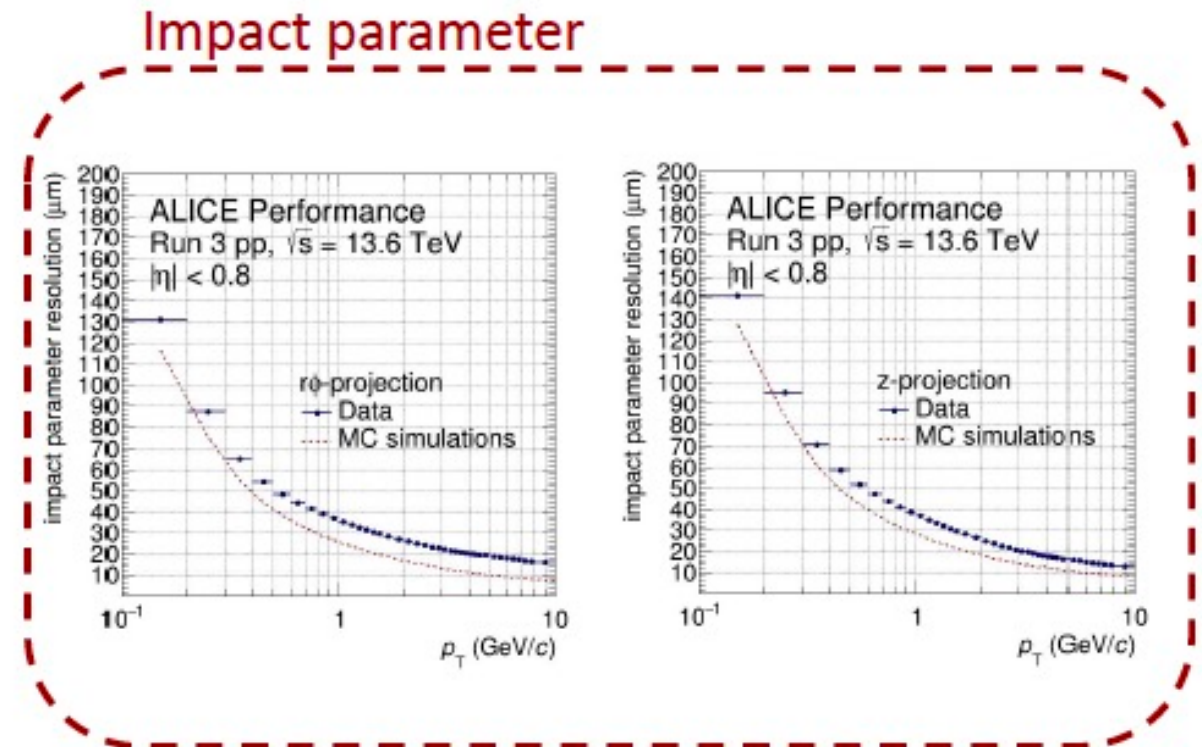
Performance results with 2022 data

Reconstruction and calibration of the 2022 pp data

1. CTF skimming on going → *free the space for the new data taking*
2. Both standard grid nodes with CPUs and the EPN farm with GPUs are being used.

Latest results on reconstructed 2022 shows that the main observable are reaching their nominal values

- *Impact parameter resolution close to the nominal values*
- dE/dx back to nominal Bethe-Bloch values
- Good reconstruction of both neutral and charged decays through EMCAL and muon systems



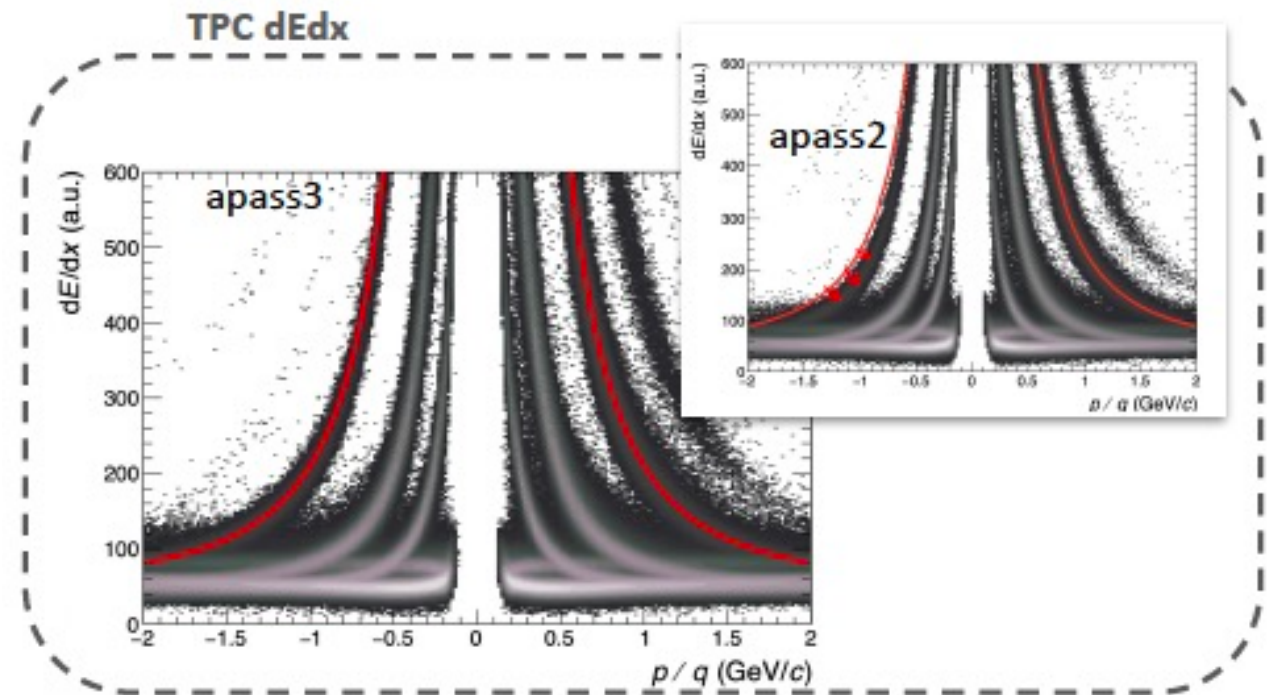
Performance results with 2022 data

Reconstruction and calibration of the 2022 pp data

1. CTF skimming on going → *free the space for the new data taking*
2. Both standard grid nodes with CPUs and the EPN farm with GPUs are being used.

Latest results on reconstructed 2022 shows that the main observable are reaching their nominal values

- Impact parameter resolution close to the nominal values
- dE/dx back to nominal Bethe-Bloch values
- Good reconstruction of both neutral and charged decays through EMCAL and muon systems



Performance results with 2022 data

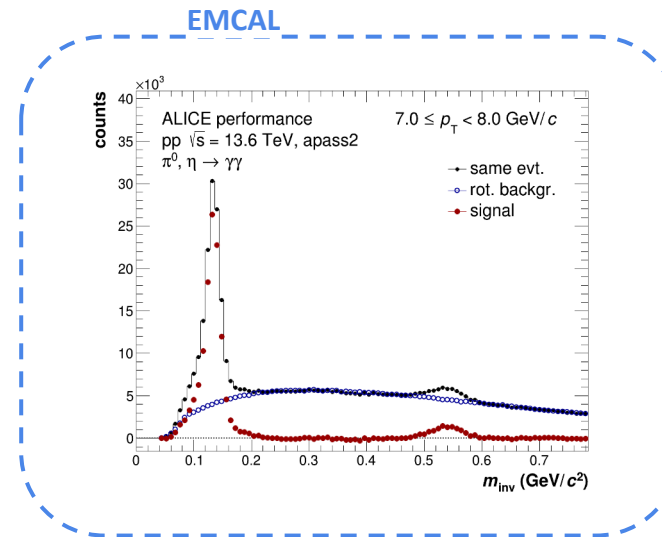
Reconstruction and calibration of the 2022 pp data

1. CTF skimming on going → *free the space for the new data taking*
2. Both standard grid nodes with CPUs and the EPN farm with GPUs are being used.

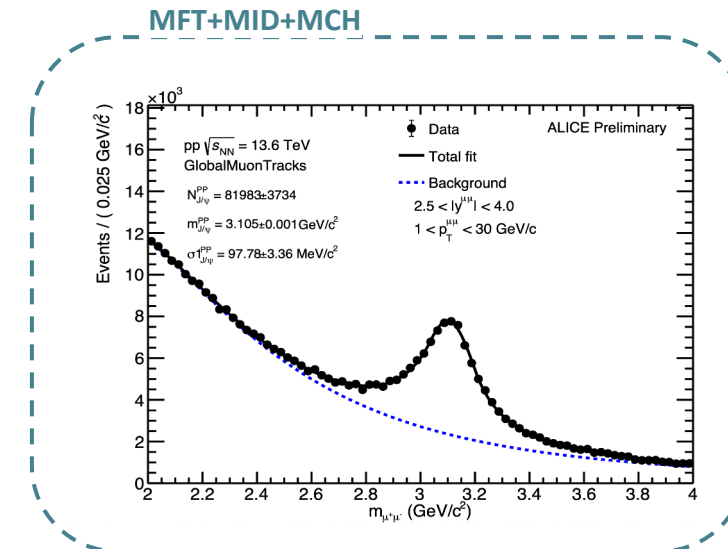
Latest results on reconstructed 2022 shows that the main observable are reaching their nominal values

- Impact parameter resolution close to the nominal values
- dE/dx back to nominal Bethe-Bloch values
- *Good reconstruction of both neutral and charged decays through EMCAL and muon systems*

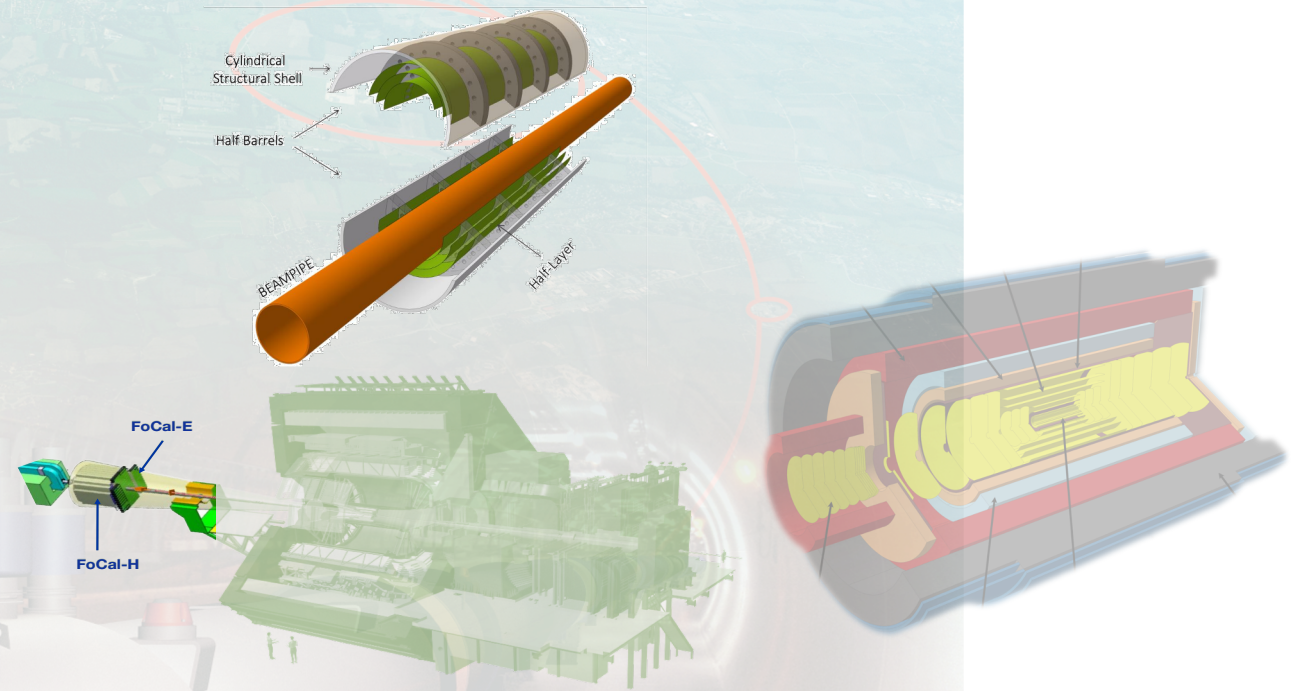
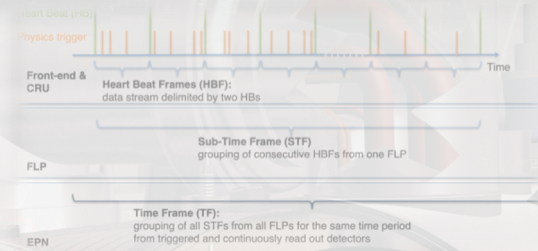
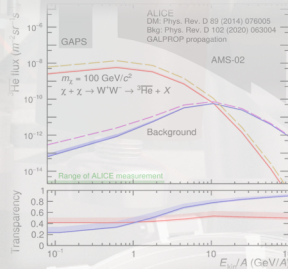
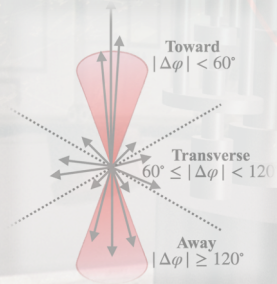
$$\pi^0, \eta \rightarrow \gamma\gamma$$



$$J/\psi \rightarrow \mu^+\mu^-$$



- 
1. Latest publications and selected physics results
 2. Data taking in 2023
 3. **ALICE + ITS3 & FoCal**
 4. ALICE 3 upgrade



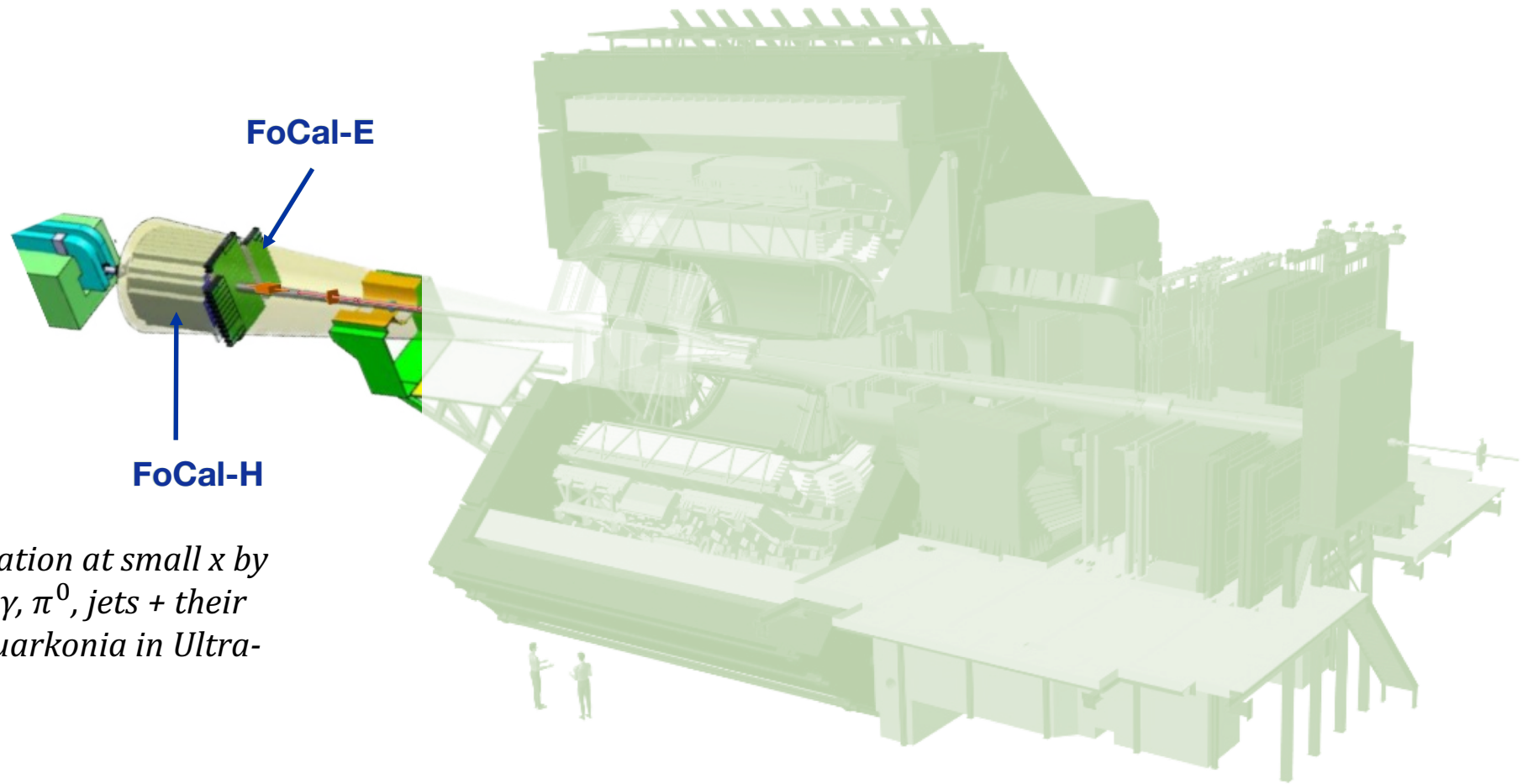
Forward Calorimeter (FoCal)

EMCal: Si-W optimized
for photon and π^0
reconstruction

HCal: Cu-scintillator:
direct photon isolation
and jets

Goals: *explore gluon saturation at small x by
measuring forward direct- γ , π^0 , jets + their
correlations in p-Pb and quarkonia in Ultra-
peripheral p-Pb and Pb-Pb*

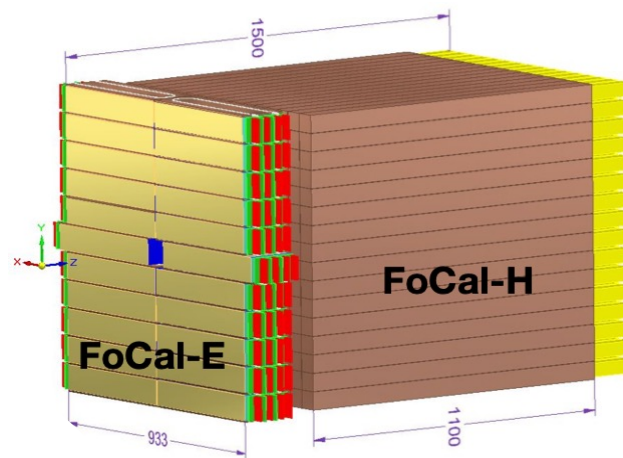
Current focus: *prototype development and beam
tests; preparation of TDR*



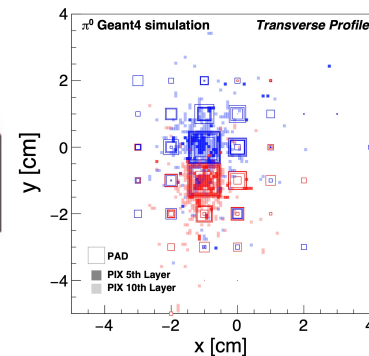
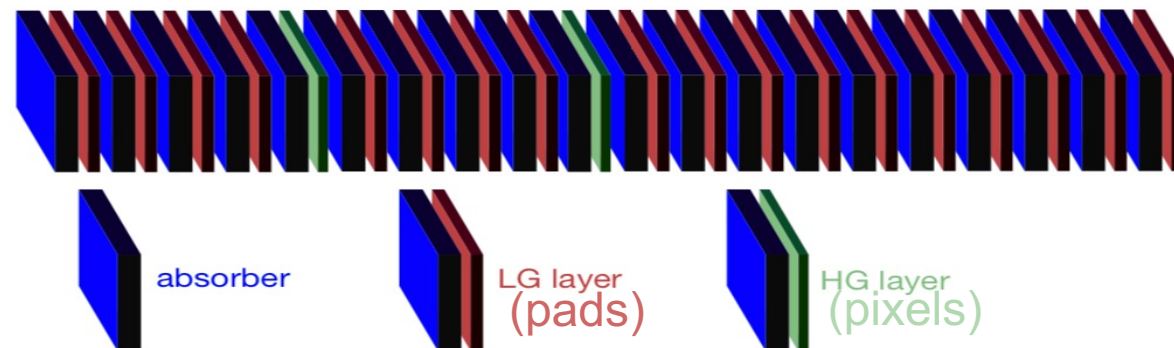
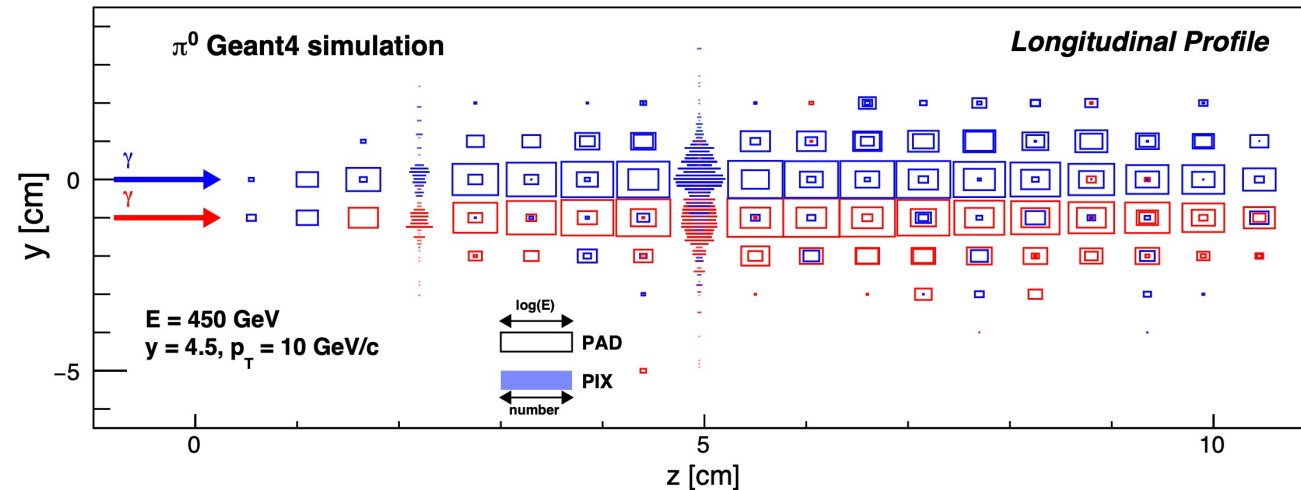
Forward Calorimeter (FoCal)

FoCal-E: segmented in 18 layers of tungsten and silicon pads with low granularity ($\sim 1 \text{ cm}^2$) and two layers of tungsten and silicon pixels with high granularity ($\sim 30 \times 30 \mu\text{m}^2$).

FoCal-H: metal/scintillating calorimeter with high granularity of up to $2.5 \times 2.5 \text{ cm}^2$



$$3.4 < \eta < 5.8$$



Letter-of-Intent:
[CERN-LHCC-2020-009](https://cds.cern.ch/record/2788812/files/CERN-LHCC-2020-009.pdf)

Forward CALorimeter (FOCAL)

Full tower prototype

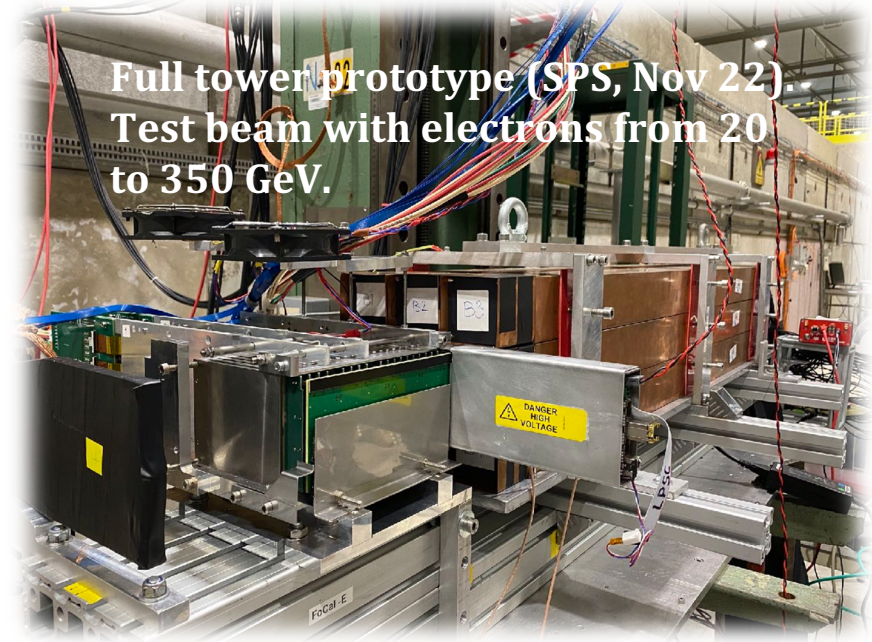
ECal

- Pads: test Time-over-Threshold for large dynamic range
- Pixels: test Outer Barrel HIC-based layers
- First time: pads + pixels with common CRU readout

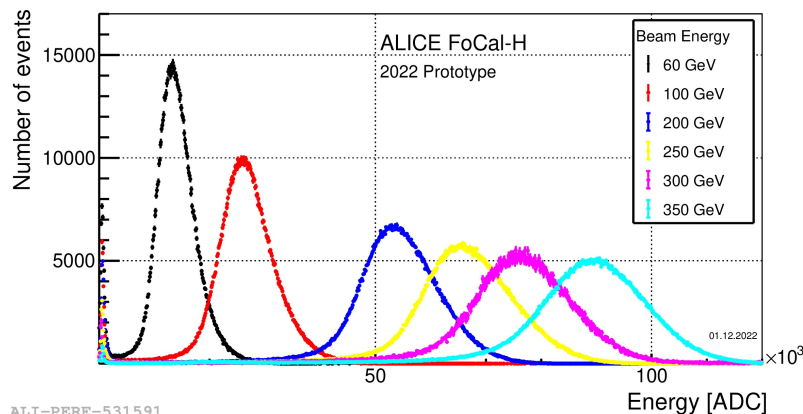
HCAL

- 9 prototype modules
- Test commercial (CAEN) and custom (VMM) readout

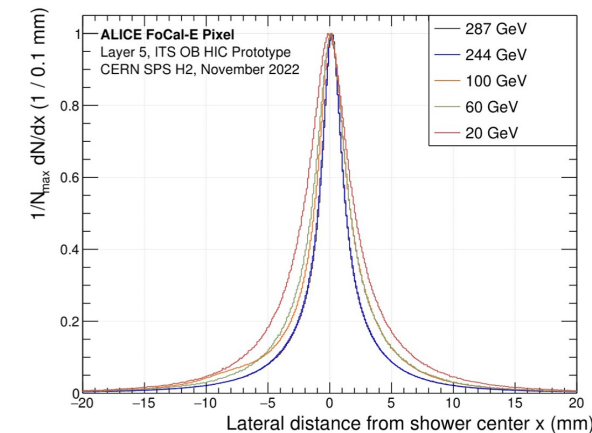
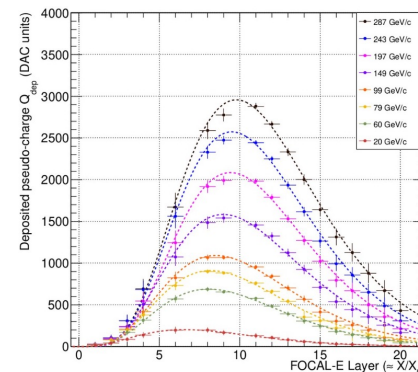
Letter-of-Intent:
[CERN-LHCC-2020-009](https://cds.cern.ch/record/2788812/files/CERN-LHCC-2020-009.pdf)



HCAL reconstructed charge distributions



Pad layers: longitudinal energy distribution



Pixel layer 5:
lateral shower
distribution

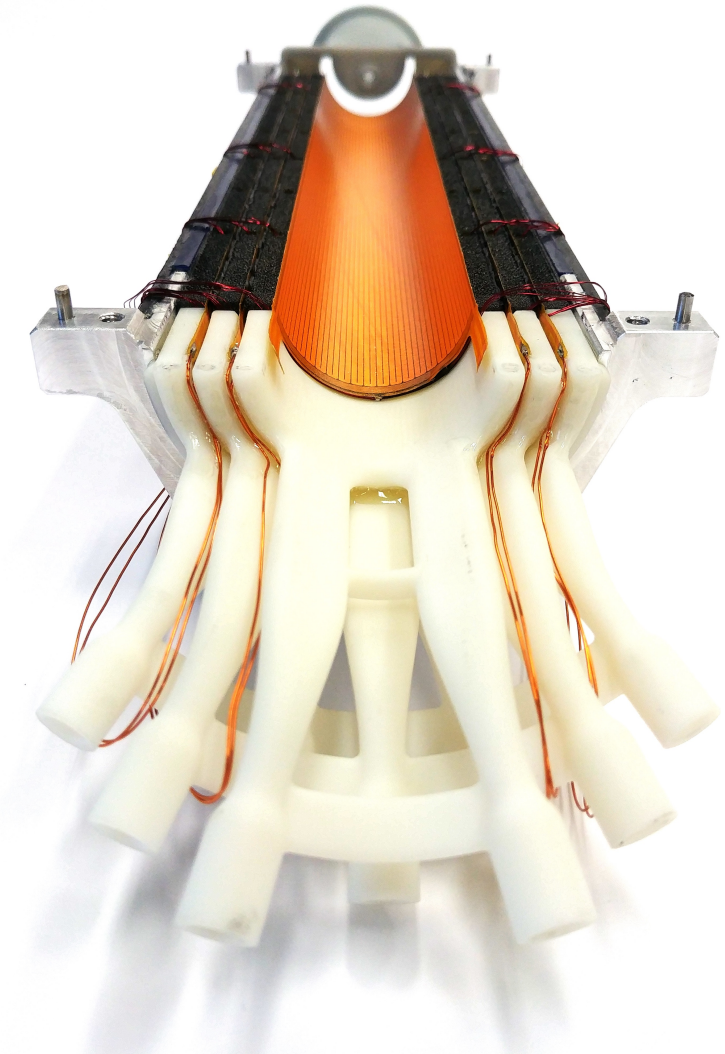
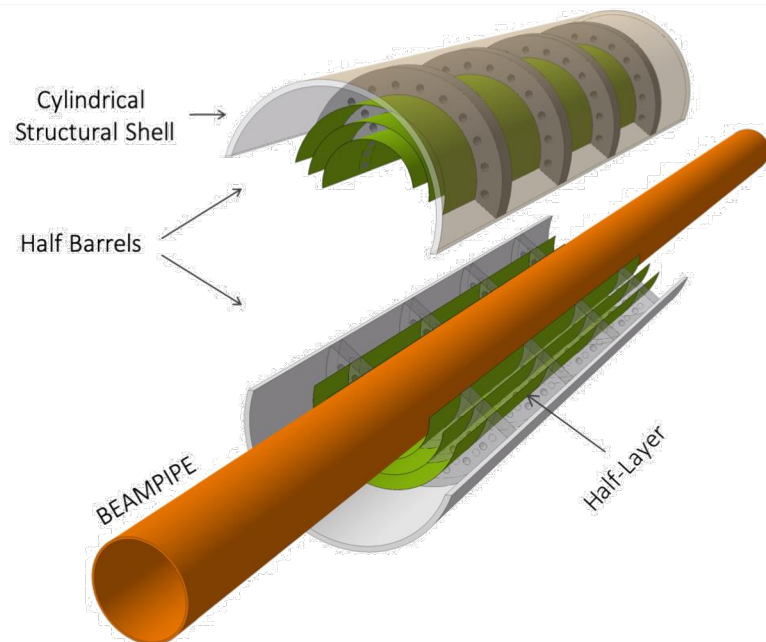
Inner Tracking System 3

Novel vertex detector:

- curved wafer-scale ultra-thin silicon sensors arranged in perfectly cylindrical layers
- unprecedented low material budget of 0.05% X_0 per layer
- innermost layer at 18 mm radial distance from the interaction point

Large improvement of the tracking precision and efficiency at low transverse momentum → significant advancement in the measurement of *low momentum charm and beauty hadrons* and *low-mass dielectrons* in heavy-ion collisions at the LHC

R&D on the detector mechanics, sensor technology and readout system ongoing.



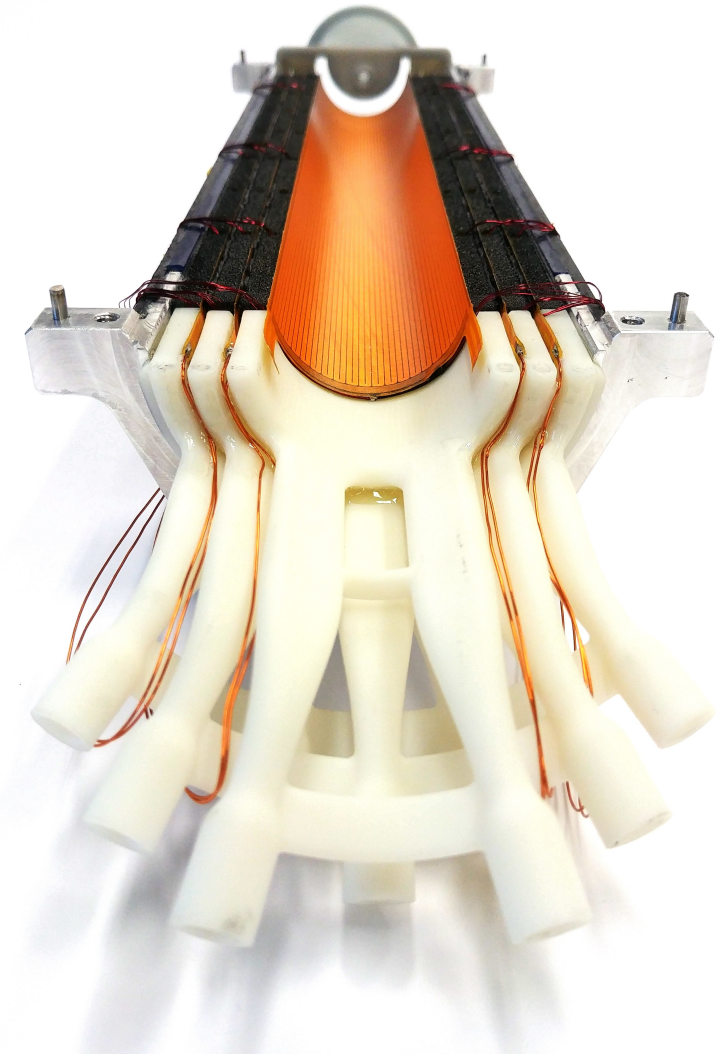
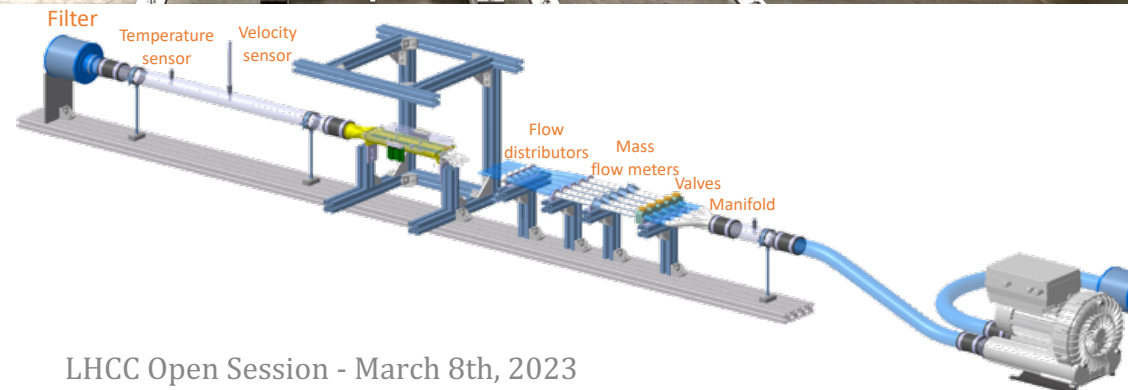
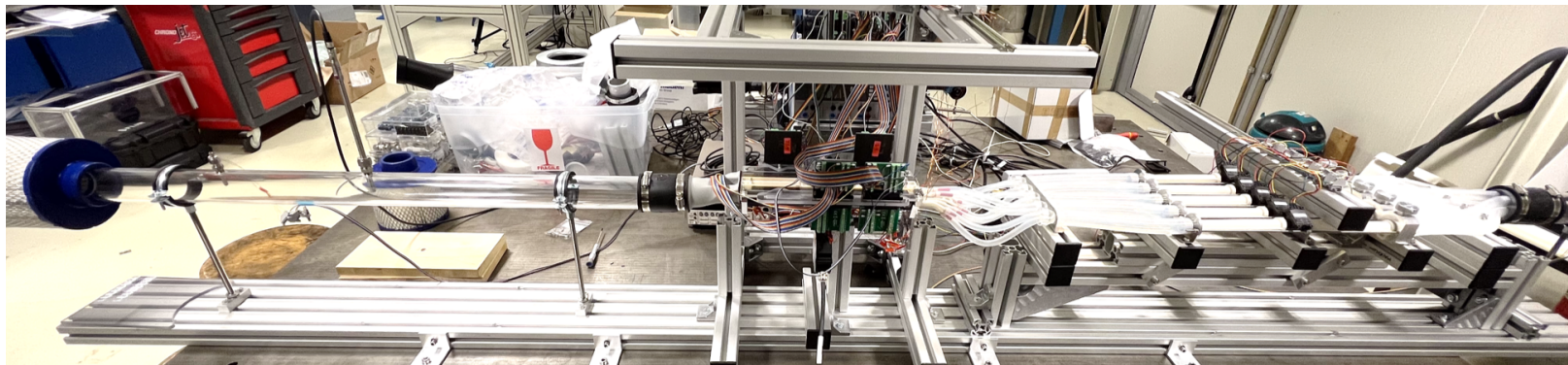
ITS3 – Breadboard model 3 + wind tunnel

Breadboard model 3 ready

- Based on silicon with added Kapton heaters
- Airducts for precise flow control

Wind tunnel commissioned

- Includes laser measurement system for vibrational analyses



ITS3 – 65nm CMOS technology

Characterisation continues at high pace

- Involves a large number of institutes (also outside ALICE)
- Beam tests at cadence of $\sim 1/\text{month}$

First comprehensive paper on the TPSCo 65nm:

- Detailed characterisation in the lab
- Several test beams
- Irradiations up to:
 $10^{15} \text{ 1MeV neq/cm}^2$ (NIEL)
and 100 kGy (TID)
(exceeding by two order of magnitude ITS3 needs)
- V2 on arXiv

Digital Pixel Test Structures implemented in a 65 nm CMOS process

Gianluca Aglieri Rinella^{a,*}, Anton Arestin^{a,o}, Roberto Baccomi^b, Paolo Braach^{a,f}, Matthew Daniel Buckland^a, Francesca Carnesecchi^a, Leonard Contin^{g,h}, Dominik Dannheim^a, Mauro Mauro^a, Jan Hasenbichler^a, He Isakov^j, Antoine Junique^a, Alexander Isakov^{a,m}, Magnus Mager^a, Lautner^{a,m}, Marius Wilk^a, Masciocchi^c, Alexandre Rachevski^b, Isabella Sanna^a, Valeri Sonneveld^p, Miljenko Usai^{n,o}, Jacob Bastiaansen^a, Matias Antonelli^h, Mauro Beollet^{d,e}, Justus Camerini^{g,h}, Paolo Camerini^{g,h}, Antonello Di Stefano^a, Artem Kashevarov^a, and 10¹⁵ 1 MeV neq cm⁻² and their detection energy resolutions were measured.

2. The DPTS chip

The Digital Pixel Test Structure (DPTS) is a MAPS produced in the first submission in TPSCo [11]. In order to optimise the technology for ionising levels of various implants in four process splits, gradual split expected to yield the best performance. To better collect the signal charge and accelerate it, similar measures to those in the 180 nm technology have been illustrated in Fig. 1(a) a deep, low-dose, n-type implant has displaced the junction from the collection diode into the epitaxial layer over the full pixel width [14]. This does not extend to the pixel border, but there is a gap in the pixel edges with the aim to increase the lateral field, pushing the collection but also to reduce charge sharing to give more operation to the larger seed pixel signal.

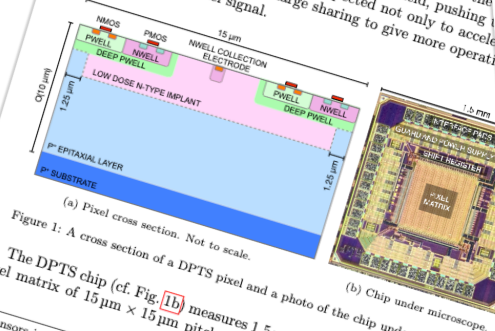


Figure 1: A cross section of a DPTS pixel and a photo of the chip under a microscope.

The DPTS chip (cf. Fig. 1(b)) measures 1.5 mm × 1.5 mm and features a 32 × 32 pixel matrix of 15 μm × 15 μm pitch, controlled by a set of external reference sensors irradiated with non-ionising, ionising, and combined doses were exposed to neutrons at JSI Ljubljana, 10 keV X-rays from a tungsten target at CERN, and 30 MeV protons at NPI Prague, respectively.

from non-irradiated to $10^{13} \text{ 1 MeV neq cm}^{-2}$ and from $10^{14} \text{ 1 MeV neq cm}^{-2}$ to $10^{15} \text{ 1 MeV neq cm}^{-2}$. In addition, at the largest irradiation dose, the four peaks are no longer resolved and the contribution from seed pixels with energy in the range of 400–1400 eV becomes more prominent. These changes to the spectrum at $10^{15} \text{ 1 MeV neq cm}^{-2}$ indicate an alteration to the charge collection mechanisms in the sensor due to radiation damage, such as the increased recombination rate and the changes in the electric fields.

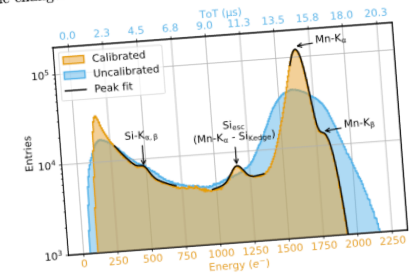


Figure 12: Measured ⁵⁵Fe spectrum of single pixel clusters with a threshold set to 120 eV. The initial spectrum (blue) is ToT calibrated (orange) which resolves the two x-ray peaks (Mn-K_α and Mn-K_β) plus the Mn-K_α silicon escape (Si_{esc}) and silicon fluorescence (Si-K_{α,β}) peaks.

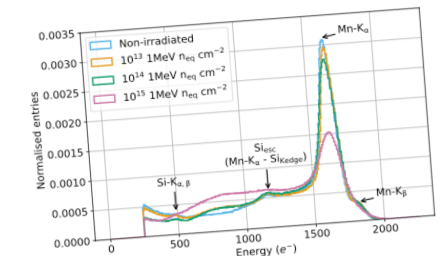


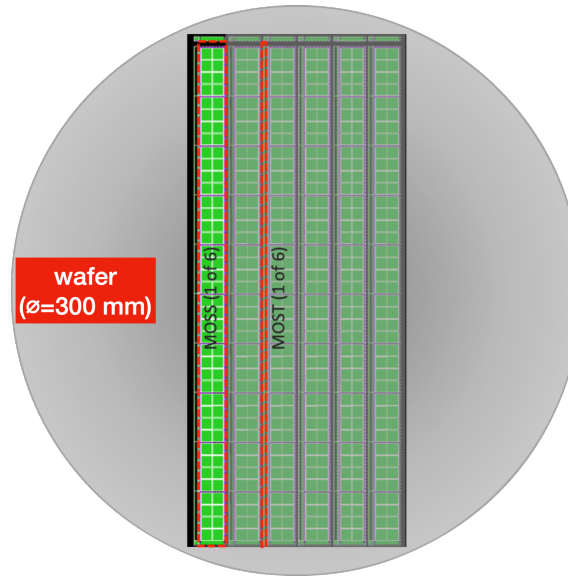
Figure 13: Measured ⁵⁵Fe spectra of seed pixels for different levels of non-ionising irradiation: non-irradiated, 10^{13} , 10^{14} and $10^{15} \text{ 1 MeV neq cm}^{-2}$.

Aglieri Rinella et al.,
[doi:10.48550/arXiv.2212.08621]

ITS3 – Engineering Run 1 (ER1)

First submission of wafer-scale sensors (stitching prototypes)

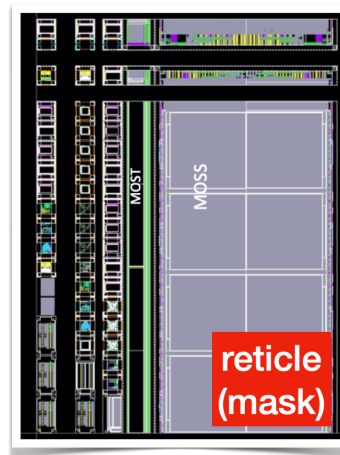
- “MOSS”: 14 x 259 mm, 6.72 MPixel (22.5×22.5 and $18 \times 18 \mu\text{m}^2$)
- “MOST”: 2.5 x 259 mm², 0.9 MPixel ($18 \times 18 \mu\text{m}^2$)



In production

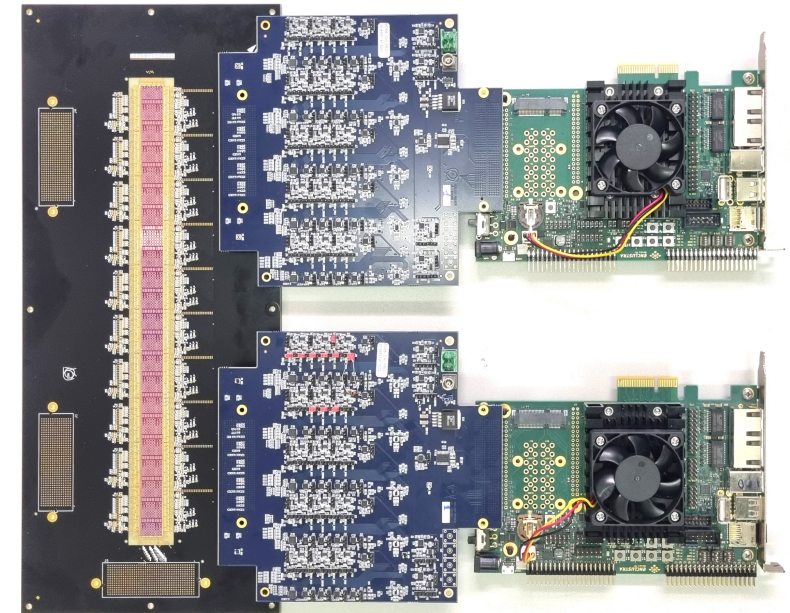
Expected shipping dates + quantities:

- Early March: delivery of dummy wafers for dicing tests
- 28 April: expected delivery of final wafers
- 1 month for thinning and dicing

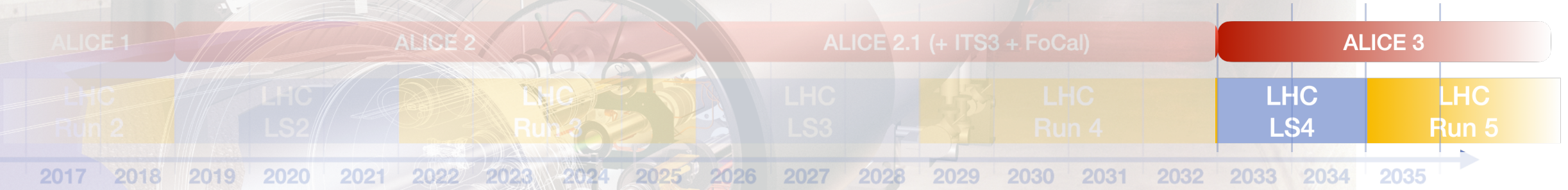
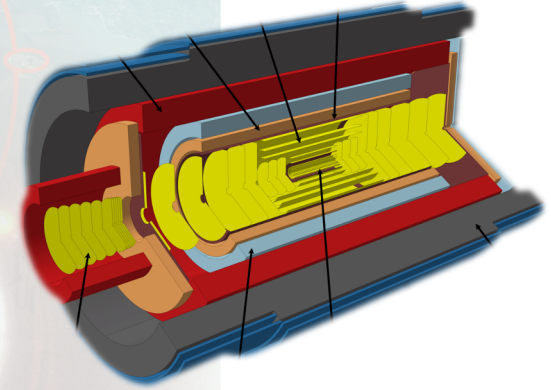
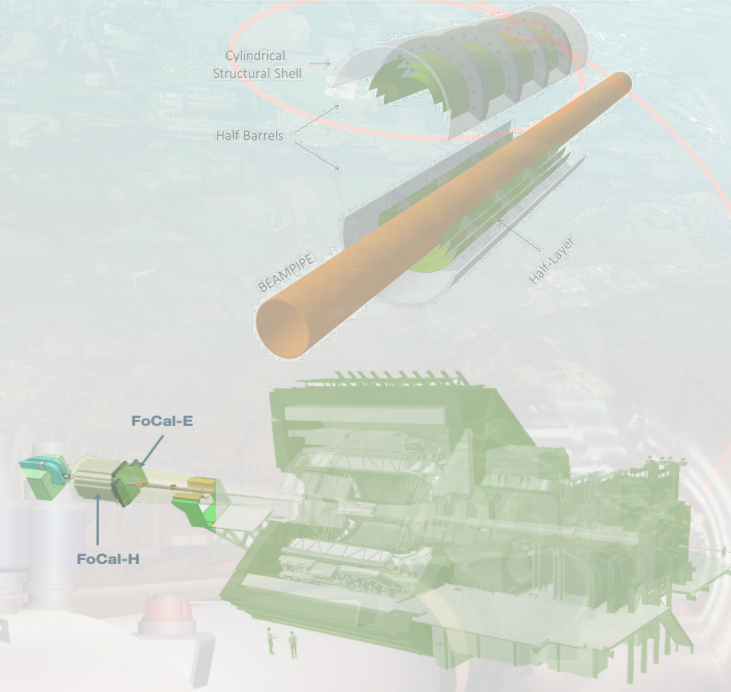
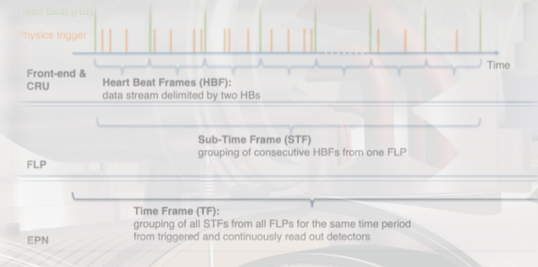
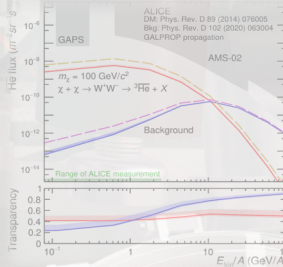
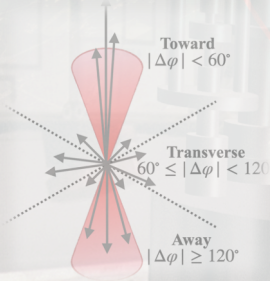


Test system for MOSS under preparation

- All parts prototyped and commissioned
- Version 2 with minor improvements being produced
- Gluing and bonding tests with dummy silicon structures
- **Ready for the chips to arrive**



1. Latest publications and selected physics results
2. Data taking in 2023
3. ALICE + ITS3 & FoCal
4. ALICE 3 upgrade



ALICE 3



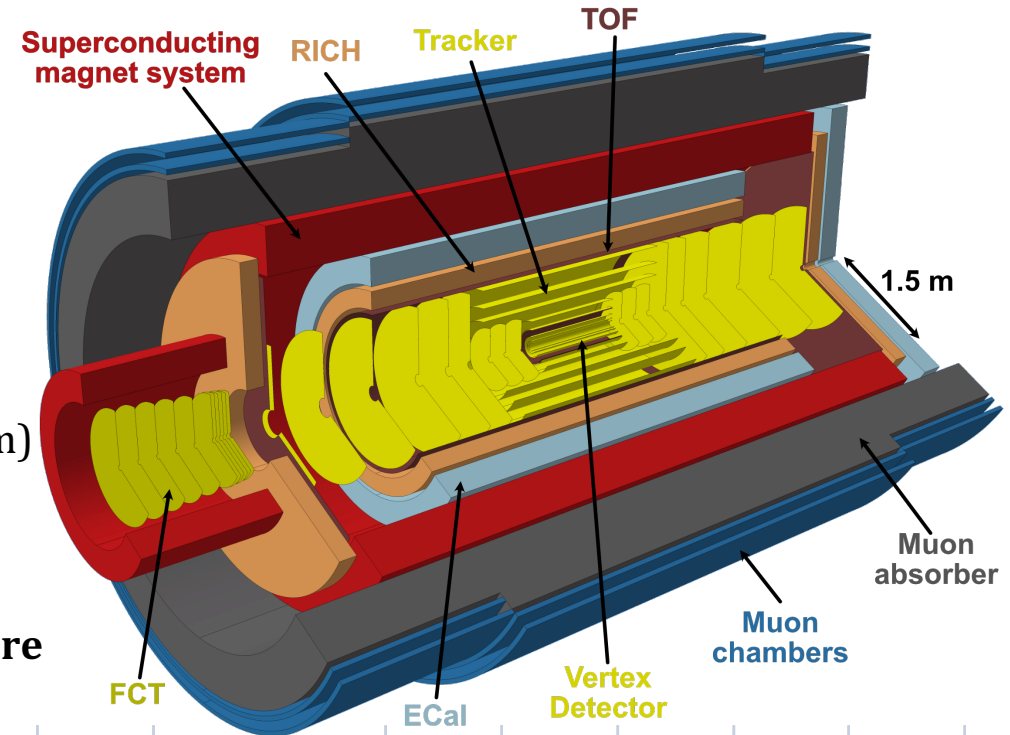
Goals:

- Quark-gluon plasma temperature and its time evolution
- Heavy flavour transport and hadronization from QGP
- Hadron interactions
- Exotica and BSM searches (axion-like particles etc.)

This will be pursued through a novel detector provided with:

- high readout rate capabilities
- unprecedented pointing resolution (innermost layer at $R=5$ mm)
- excellent tracking and particle identification over a large acceptance

Preparation of scoping document as part of approval procedure for phase IIb upgrades (Q4 '23 - Q1 '24)



ALICE 3: R&D on Time-Of-Flight

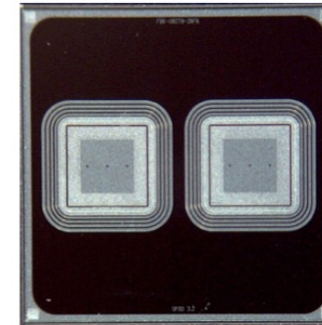
1. Thinner LGAD sensors

- 25 and 35 μm thick prototypes
- Excellent time resolution < 25 ps
- Sensors of 10 μm in preparation

First very thin LGAD prototypes
produced by FBK

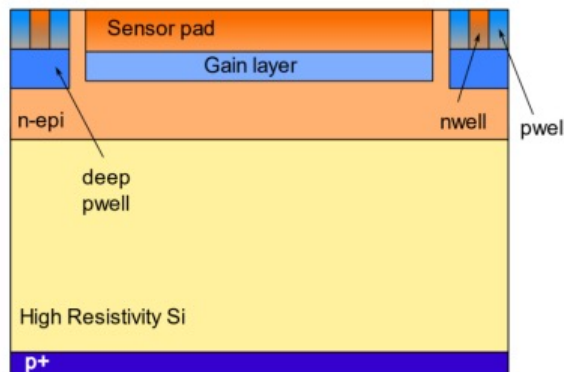
25 μm and **35 μm** -thick
FBK single channel

Area = 1x1 mm²



2. CMOS sensors with gain layer

- Sensors back from foundry
- Preparations for test beams



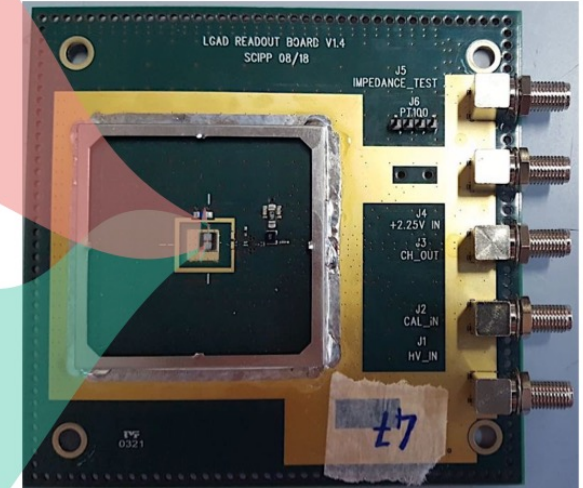
Standard sensors produced by HPK

50 μm -thick HPK
single channel
(W42 & W36 with different
doping concentrations)

Area = 1.3x1.3 mm²



SantaCruz single-channel LGAD
read-out board V1.4 SCIPP
08/18 ($G_{\text{amplifier}} \sim 6$)



+ Second stage external amplifier
($G_{\text{amplifier}} \sim 11-14$)

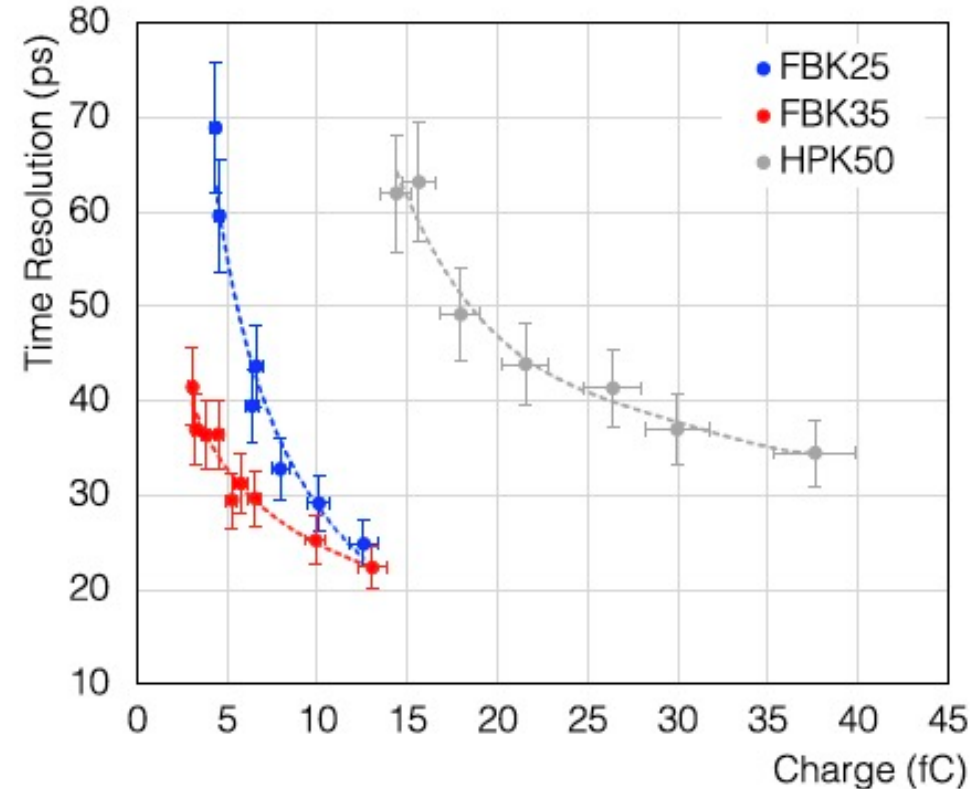
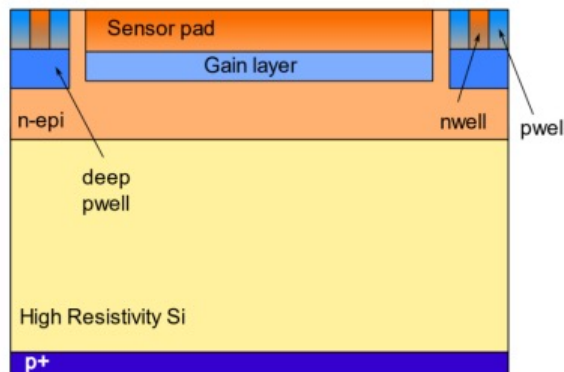
ALICE 3: R&D on Time-Of-Flight

1. Thinner LGAD sensors

- 25 and 35 μm thick prototypes
- Excellent time resolution < 25 ps
- Sensors of 10 μm in preparation

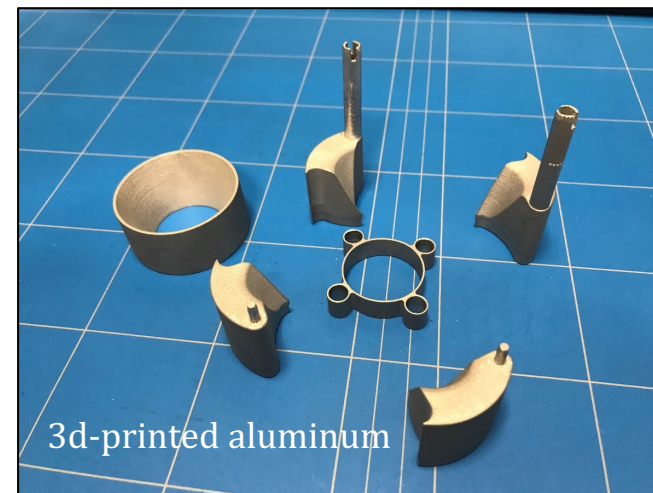
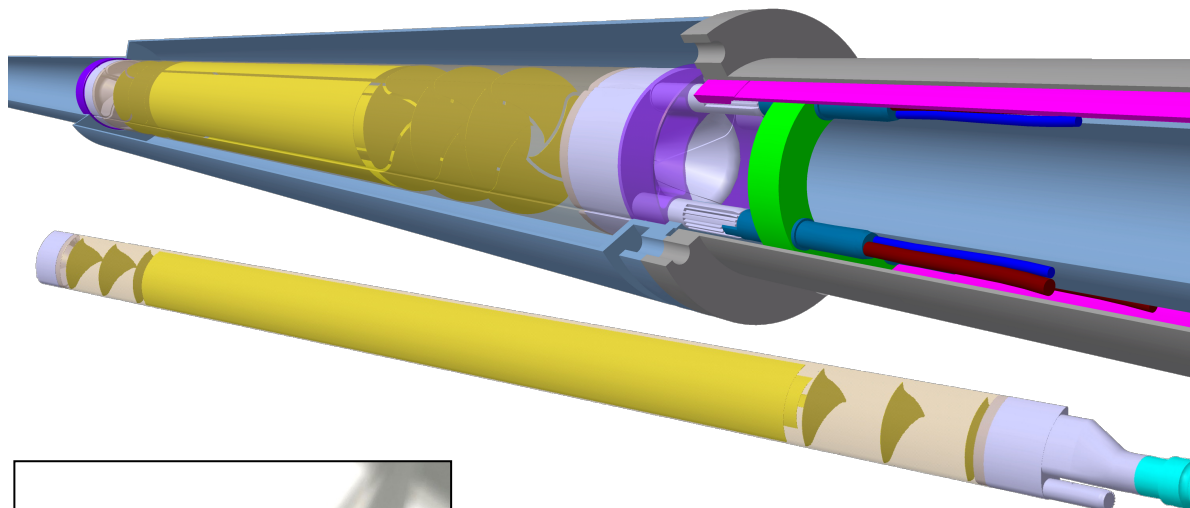
2. CMOS sensors with gain layer

- Sensors back from foundry
- Preparations for test beams

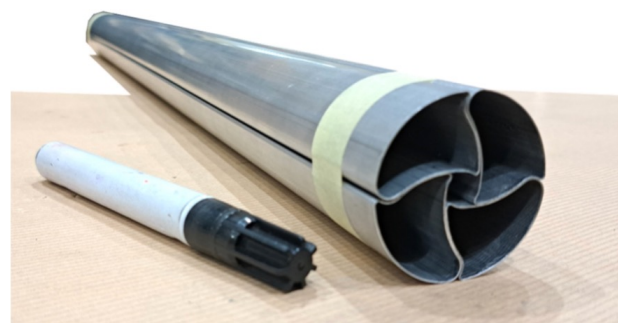
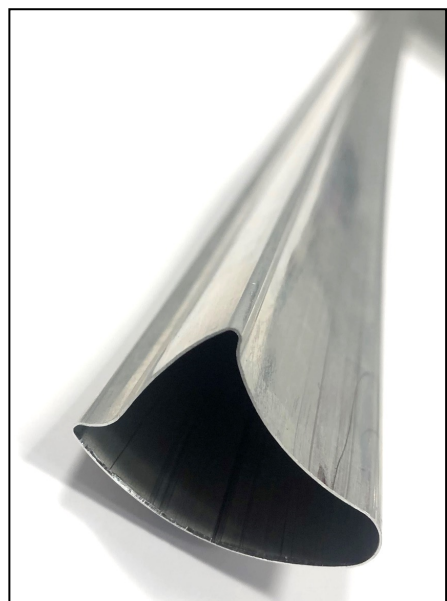


[F. Carnesecchi et al.,
https://doi.org/10.1140/epjp/s13360-022-03619-1](https://doi.org/10.1140/epjp/s13360-022-03619-1)

ALICE 3: R&D on vertex detector mechanics



Module mock-up: 0.3mm Aluminum foil welded and formed

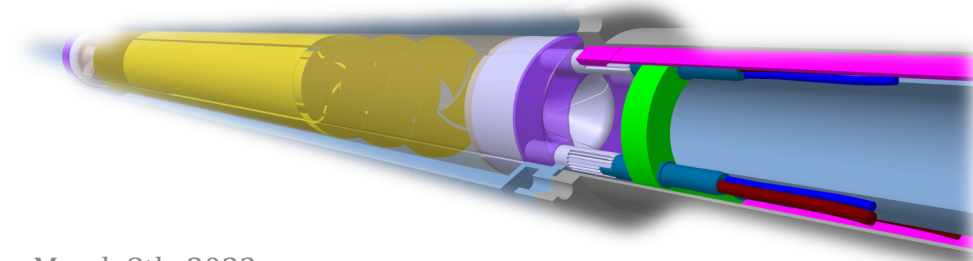
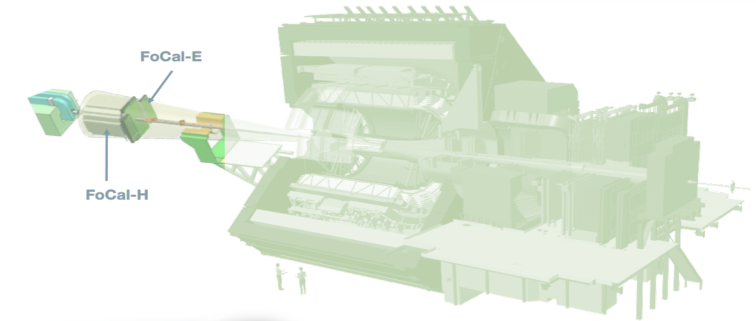
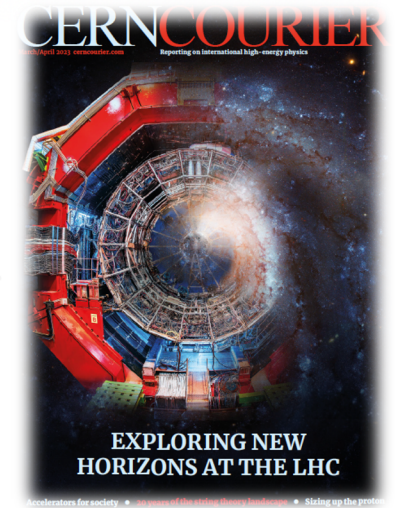
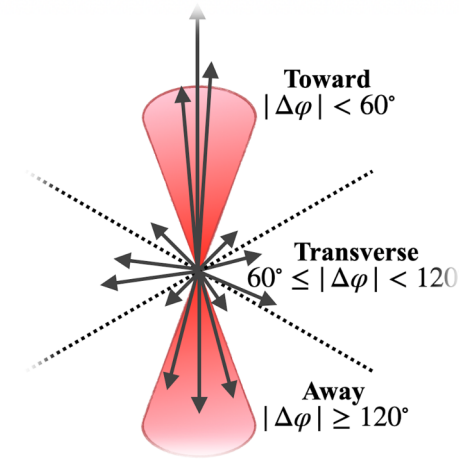


extruded aluminium (*procedure also used in beampipe*)



Conclusions

1. Since the last LHCC ALICE published 16 new papers, including an overview of the ALICE upgrade during the Long Shutdown 2
2. Preparation of 2023 data taking ongoing: activities already planned for pp runs, where also preparatory tests for Pb-Pb will be organized
3. ITS3 and FoCal: Intense prototype testing in lab and with beams ongoing; TDRs in preparation.
4. ALICE 3: R&D in progress for sub-detector systems.

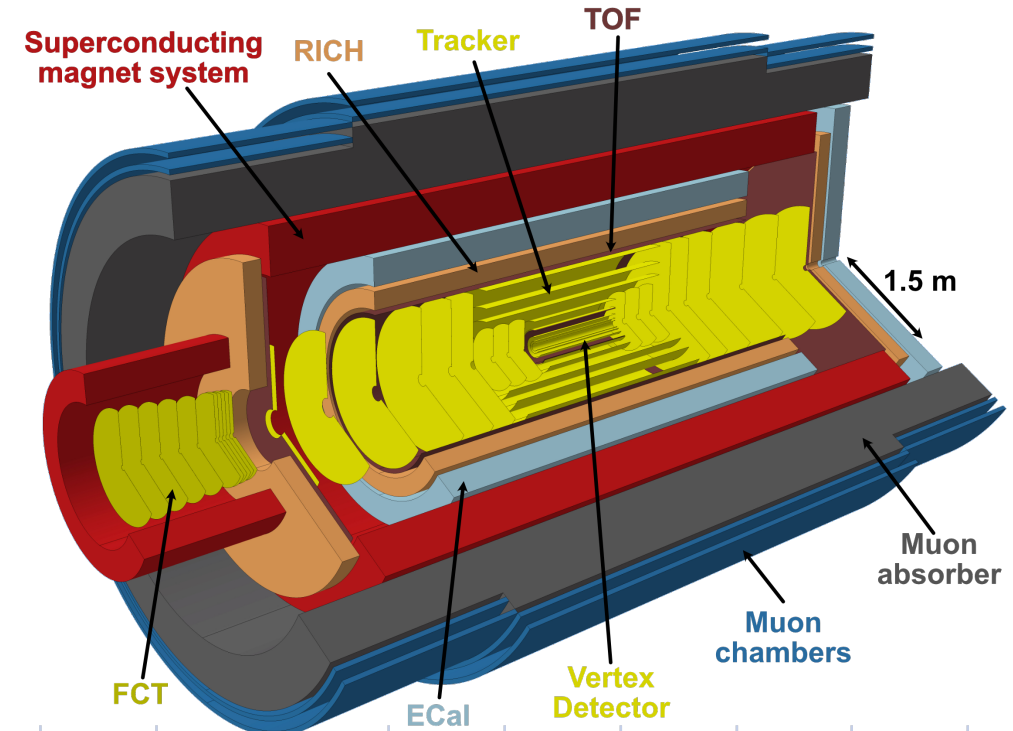


backup

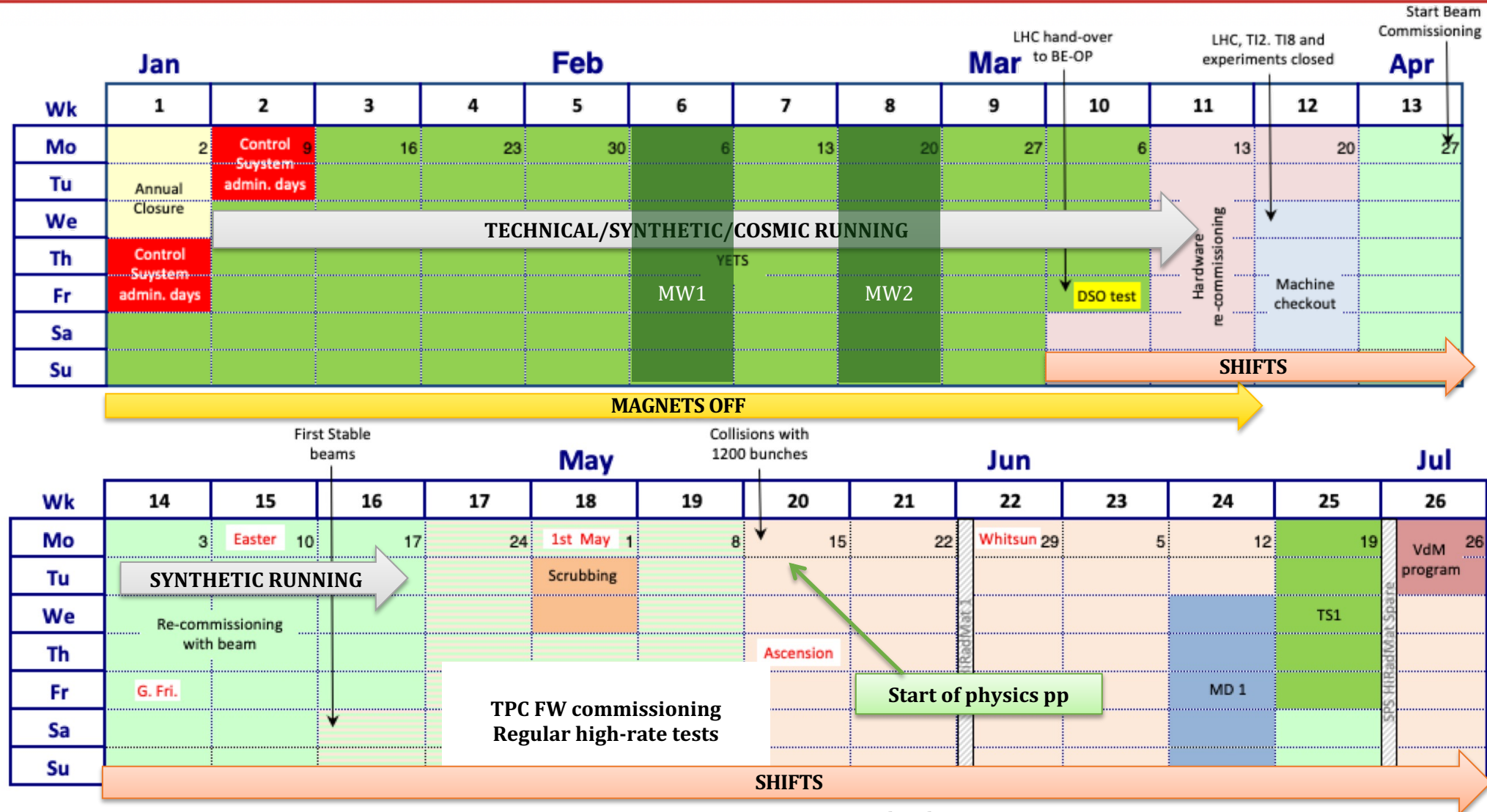
ALICE 3



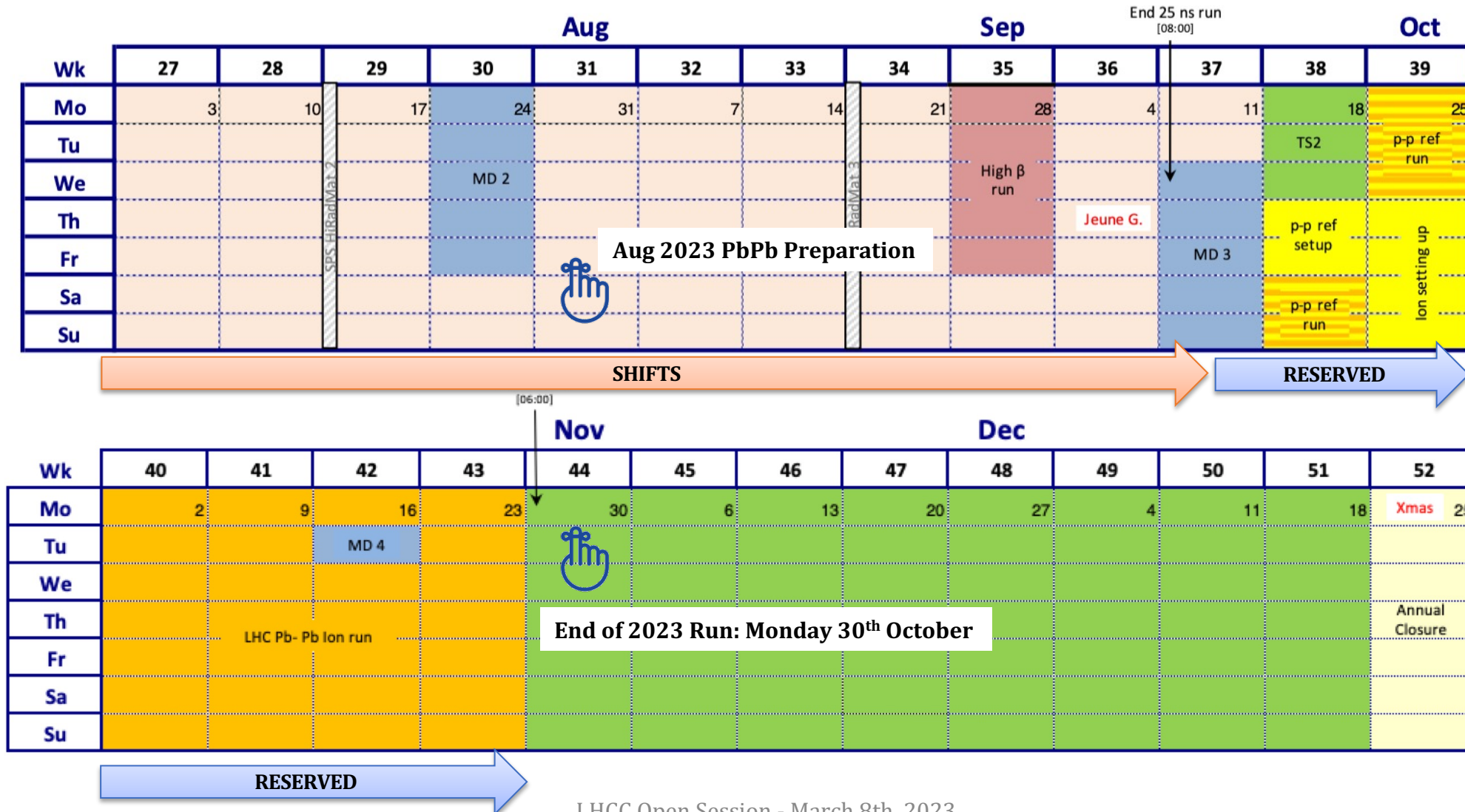
- Preparation of scoping document as part of approval procedure for phase IIb upgrades (Q4 '23 - Q1 '24)
- 2023-25: *R&D for the selection of technologies*, small-scale proof of concept prototypes
- 2026-27: large-scale engineered prototypes → Technical Design Reports
- 2028-30: construction and testing
- 2031-32: contingency
- 2033-34: preparation of cavern and installation



2023 LHC schedule and ALICE plans

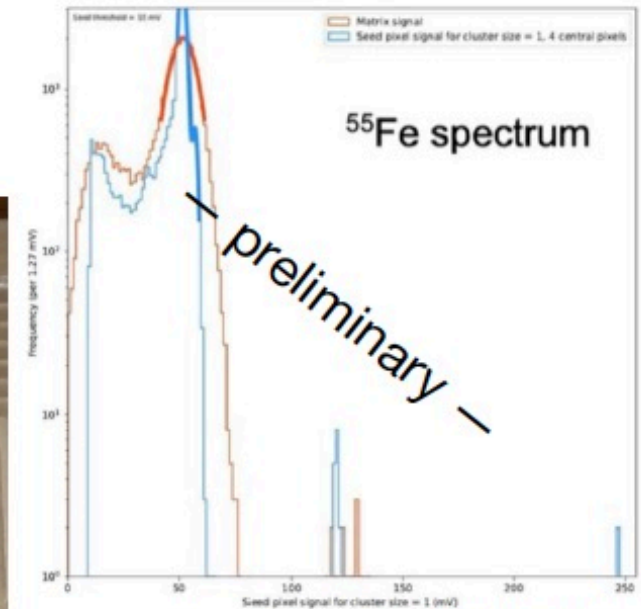
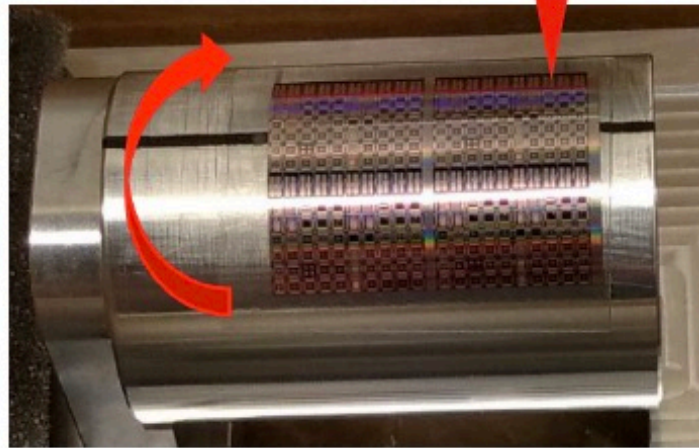
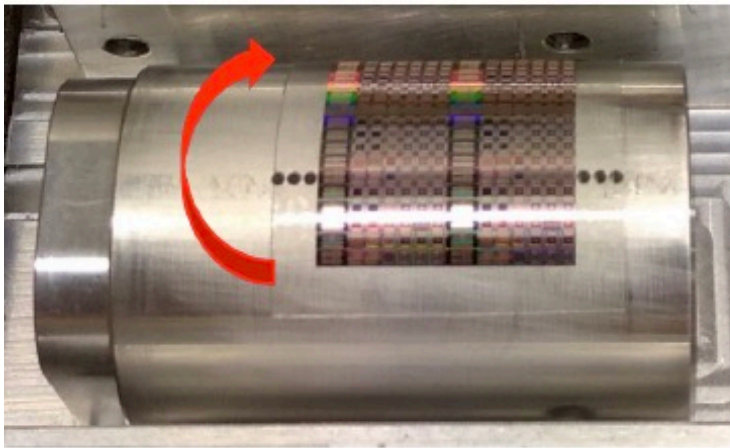


2023 LHC schedule and ALICE plans



ITS3 – 65nm CMOS technology

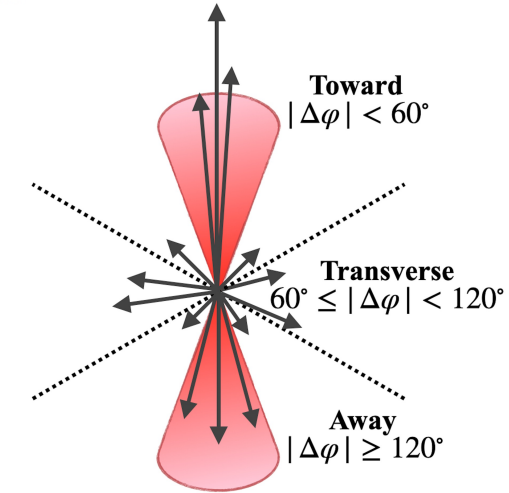
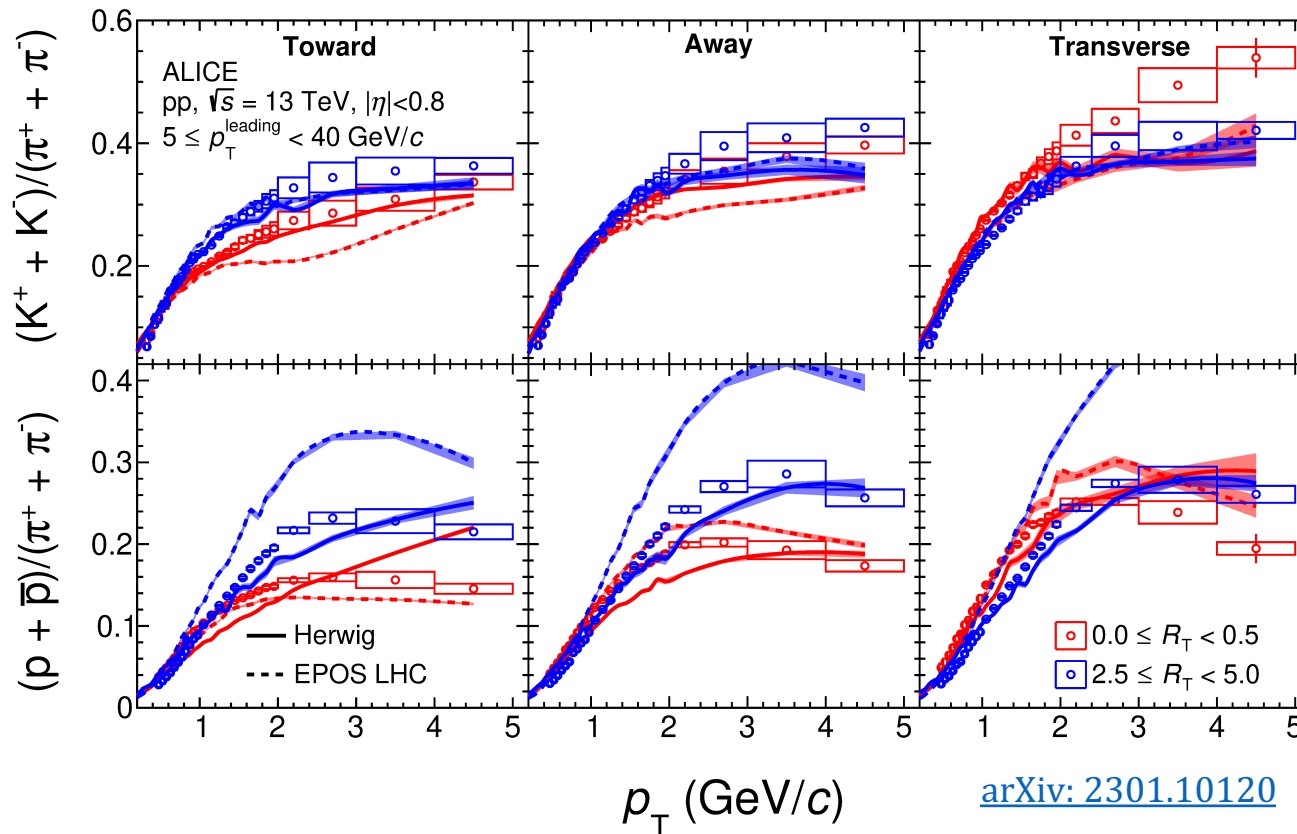
- ▶ Larger pieces from fully processed 65nm wafers are bent to $R = 18$ mm and electrically characterised
- ▶ They work nicely (tested with a Fe-55 source)
- ▶ More comprehensive study ongoing



Magnus Mager (CERN) | ITS3 | LHCC | 07.03.2023 | 9

Identified particle production vs. R_T

Relative transverse activity classifier: $R_T = N_{ch}^{transverse} / \langle N_{ch}^{transverse} \rangle$



K/π ratio: different behaviours in transverse compared to toward and away sides

p/π ratio: radial flow-like features for high R_T

HERWIG: does not reproduce the p_T dependence for the p/π ratio

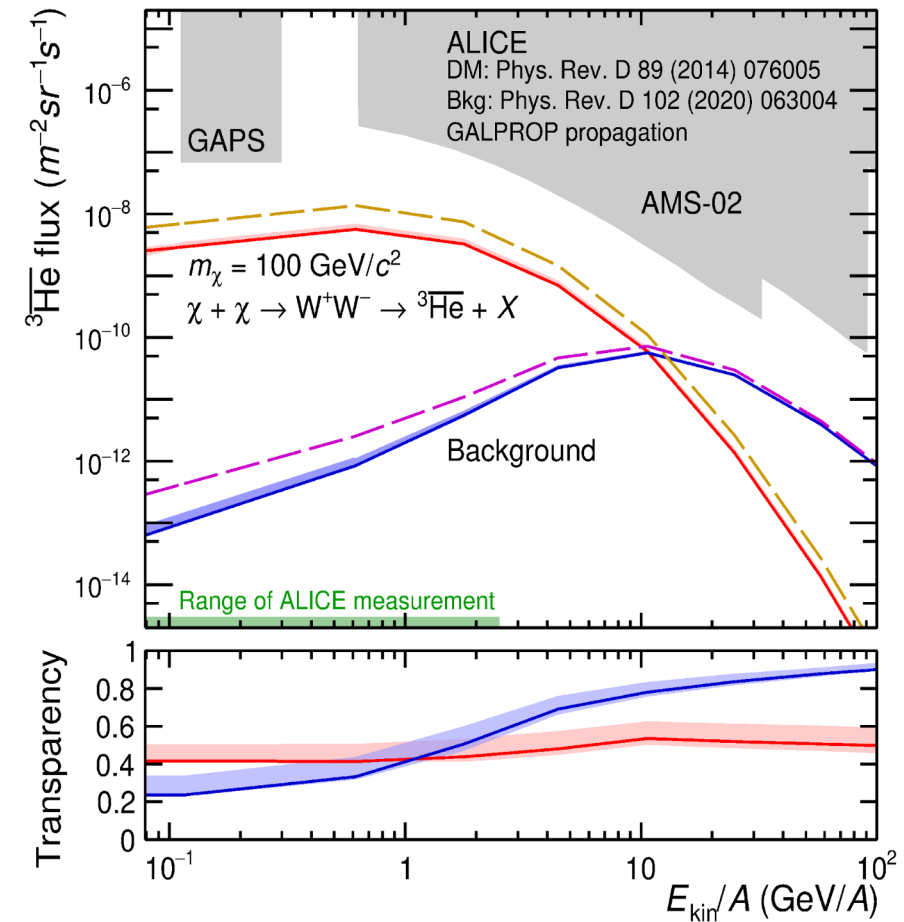
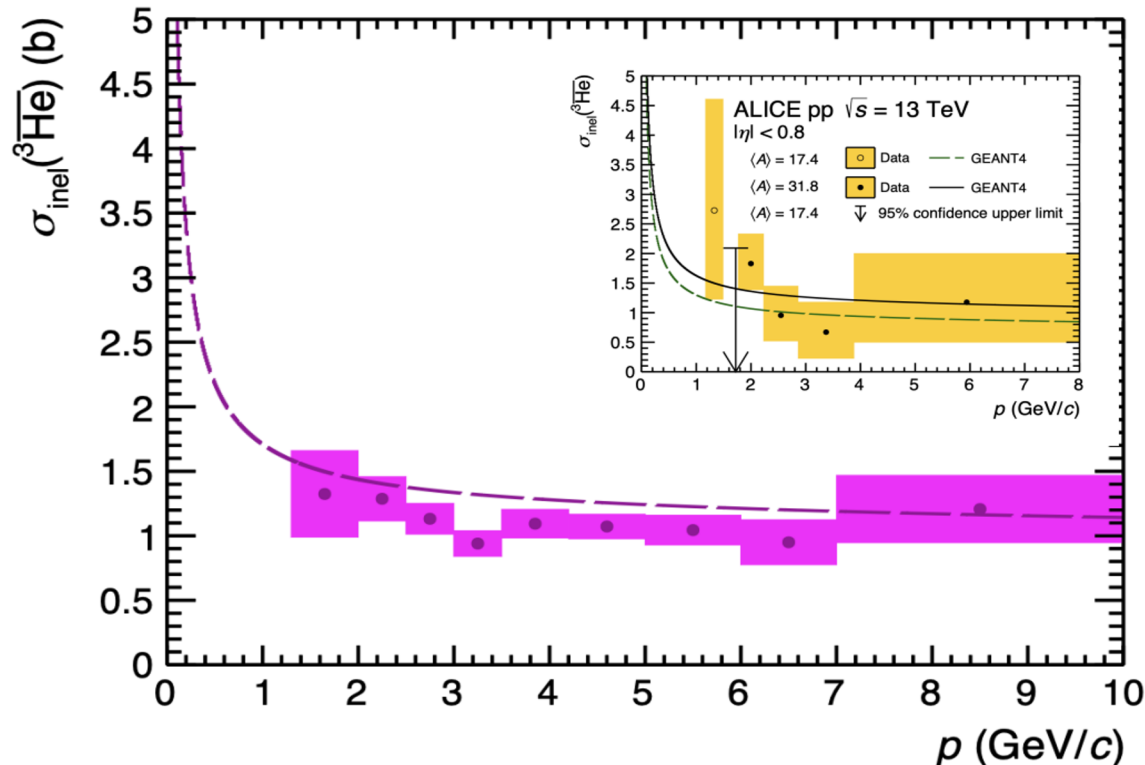
EPOS LHC: does predict but overestimates the evolution with R_T

anti-3He nuclei absorption and impact on their propagation in the Galaxy

Nature Physics: <https://www.nature.com/articles/s41567-022-01804-8>



- First ever measurement of antihelium-3 inelastic cross sections
- High transparency of 50% for typical DM scenario and 25-90% for background
- Antihelium is a promising candidate for dark matter searches!

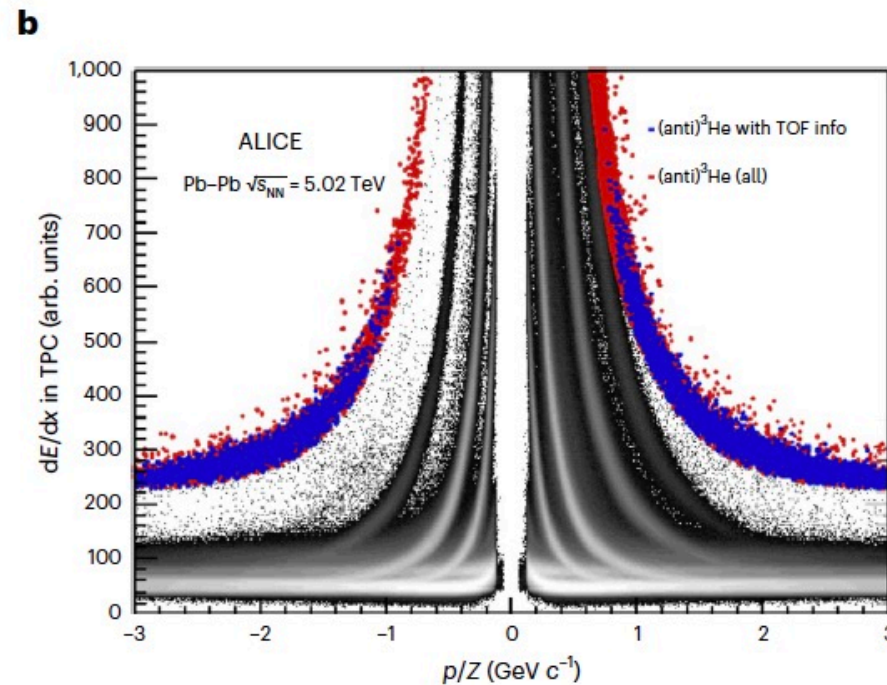
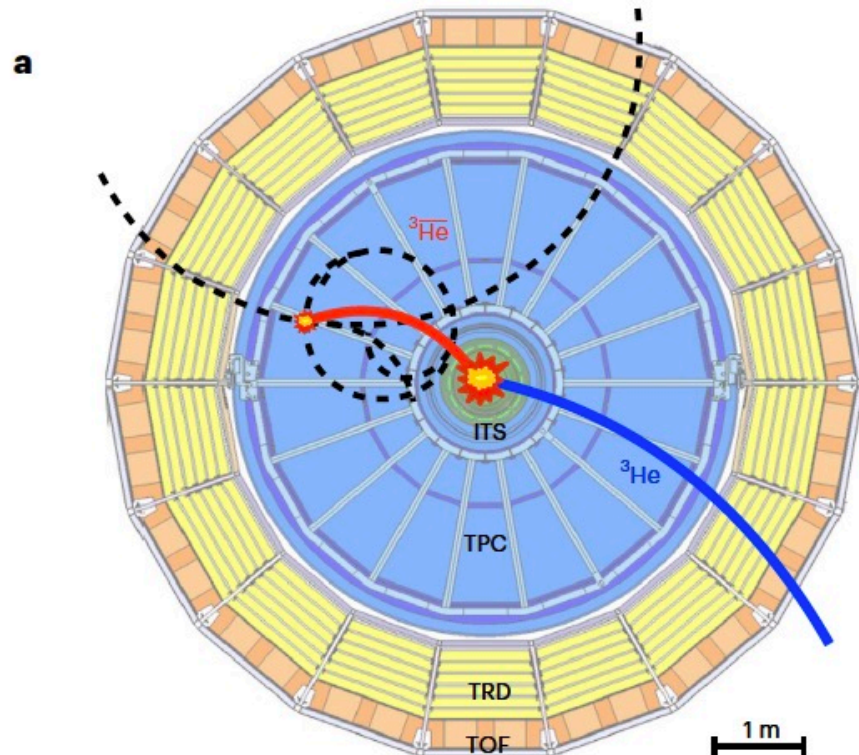


ALI-PUB-532060

anti- ^3He nuclei absorption and impact on their propagation in the Galaxy

Nature Physics: <https://www.nature.com/articles/s41567-022-01804-8>

- First ever measurement of antihelium-3 inelastic cross sections
- High transparency of 50% for typical DM scenario and 25-90% for background
- Antihelium is a promising candidate for dark matter searches!

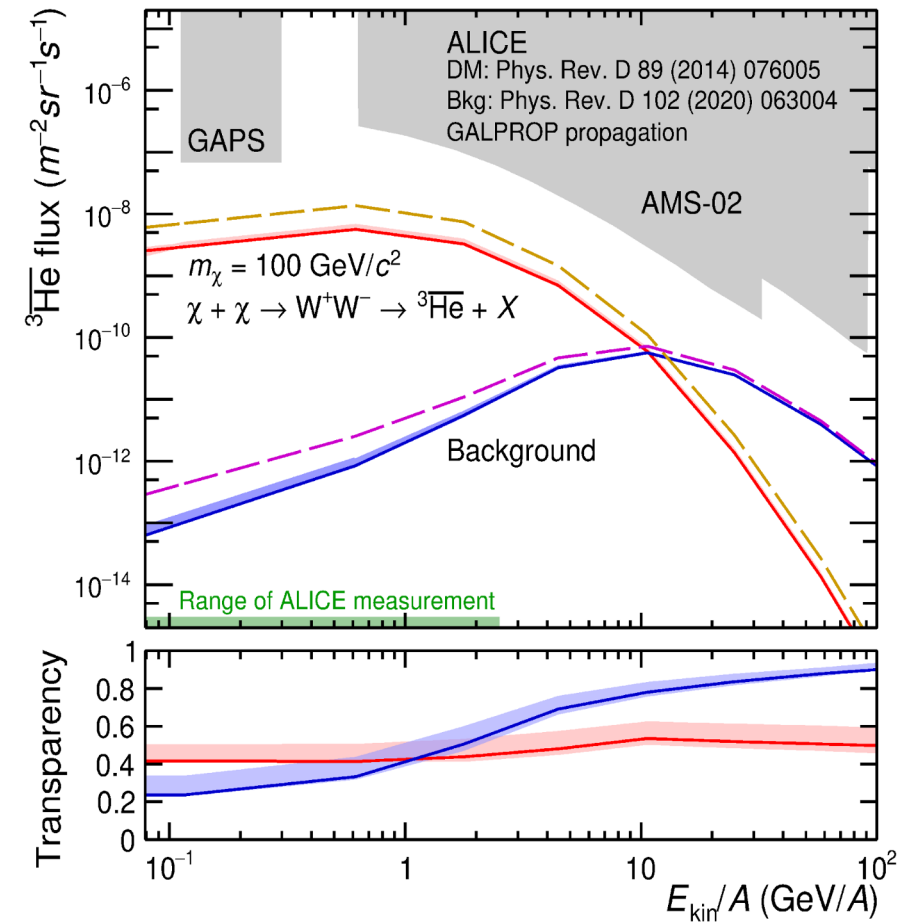
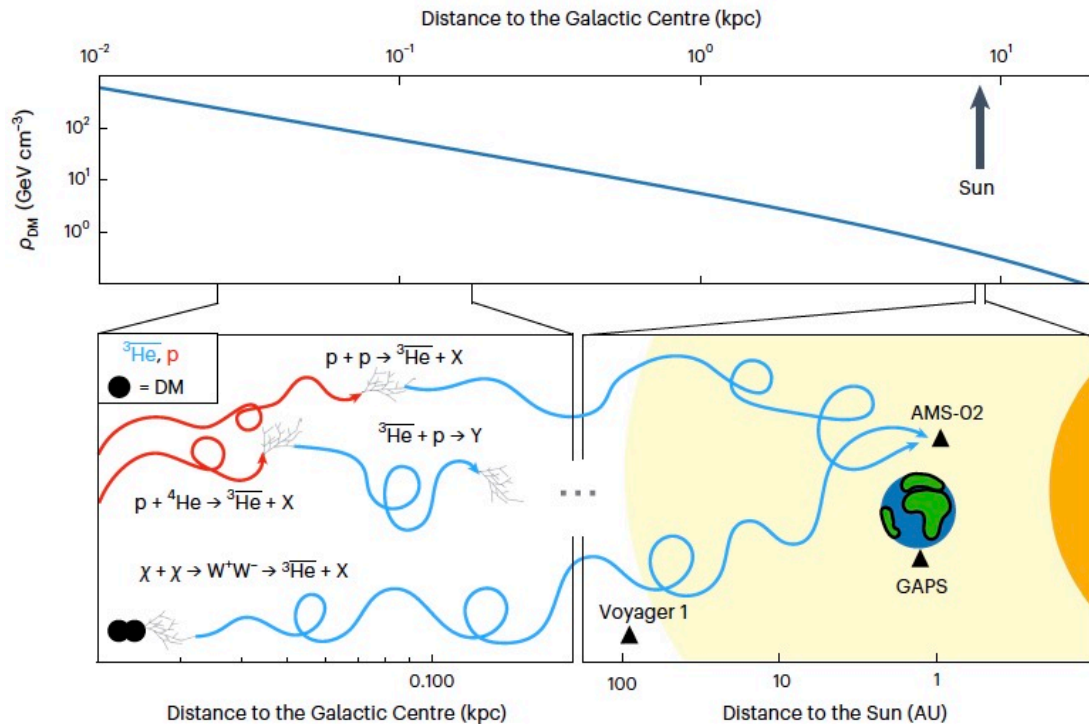


anti-3He nuclei absorption and impact on their propagation in the Galaxy

Nature Physics: <https://www.nature.com/articles/s41567-022-01804-8>



- First ever measurement of antihelium-3 inelastic cross sections
- High transparency of 50% for typical DM scenario and 25-90% for background
- Antihelium is a promising candidate for dark matter searches!



ALI-PUB-532060

anti-3He nuclei absorption and impact on their propagation in the Galaxy

Nature Physics: <https://www.nature.com/articles/s41567-022-01804-8>

